Solution of the Kwieciński evolution equations for unintegrated parton distributions using the Mellin transform

Enrique Ruiz Arriola*
Departamento de Física Moderna, Universidad de Granada, E-18071 Granada, Spain

Wojciech Broniowski†
H. Niewodniczański Institute of Nuclear Physics, Polish Academy of Sciences, PL-31342 Kraków, Poland
(Received 1 April 2004; published 18 August 2004)

The Kwieciński equations for QCD evolution of unintegrated parton distributions in transverse-coordinate space (b) are analyzed with the help of the Mellin-transform method. The equations are solved numerically in the general case, as well as in a small-b expansion which converges fast for $b\Lambda_{\rm QCD}$ sufficiently small. We also discuss the asymptotic limit of large bQ and show that the distributions generated by the evolution decrease with b according to a power law. Numerical results are presented for the pion distributions with a simple valencelike initial condition at the low scale, following from chiral large-N_c quark models. We use two models: the spectral quark model and the Nambu–Jona-Lasinio model. Formal aspects of the equations, such as the analytic form of the b-dependent anomalous dimensions, their analytic structure, as well as the limits of unintegrated parton densities at $x\to 0$, $x\to 1$, and at large b, are discussed in detail. The effect of the spreading of the transverse momentum with increasing scale is confirmed, with $\langle k_\perp^2\rangle$ growing asymptotically as $Q^2\alpha(Q^2)$. Approximate formulas for $\langle k_\perp^2\rangle$ for each parton species are given, which may be used in practical applications.

DOI: 10.1103/PhysRevD.70.034012 PACS number(s): 12.38.Aw, 12.38.Bx, 14.40.Aq

I. INTRODUCTION

The *unintegrated* parton distributions (UPDs) have been considered in numerous works on applications of perturbative QCD [1–16]. These distributions are generalizations of the usual integrated parton distributions (PDs) and in some sense more basic objects, as PDs are obtained from UPDs by integration over the transverse momentum of the parton. The notion of UPDs relies on the $k_\perp$ factorization and, in the spirit of the CCFM equations [17–20], introduces two scales: the probing scale Q and the transverse-momentum scale $k_\perp$. Recently, the UPDs have gained substantial attention, since they enter many exclusive physical processes, such as the production of the Higgs boson [21,22], the W boson [23], heavy flavors [21,24–27], jet production [21,28], particle production [29], or hadron production in relativistic heavy-ion collisions [30,31]. The unintegrated distributions were also used in studies of the longitudinal [32], charmed [33], and spin [34,35] structure functions of the nucleon, as well as analyzed in the dipole picture of QCD [36]. Thus, UPDs are needed for phenomenological studies, although admittedly the traditional colinear factorization approach explains most of the currently available data. Moreover, effects of resummations or partonic thresholds are important in extensions of the theoretical techniques.

The UPDs, similarly to other entities in QCD, undergo evolution with the change of the probing scale Q. The philosophy adopted here is similar to the case of the integrated PDs. At some initial scale Q_0 we need to know the nonperturbative quantity from measurements, models, or lattice calculations, and then we can evolve it to a different scale Q with the help of suitable QCD evolution equations. In the case of integrated PDs we need to assume the dependence of PDs on the Bjorken x variable at the initial scale Q_0. For the UPDs we need to know in addition the dependence on the transverse momentum $k_\perp$ or, equivalently, the transverse coordinate b, which is the variable Fourier-conjugated to $k_\perp$. Knowing this, we compute, with no extra physical input apart for the assumptions entering the QCD evolution, the unintegrated distribution at the final scale Q.

Important physics questions may be answered. In particular, the UPDs evolve in such a way that the average transverse momentum increases in a specified way with the scale [14–16,21]. This spreading can be studied quantitatively within the approach. This constrains the freedom in phenomenological analyses of processes involving the UPDs.

In his studies of the problem, Kwieciński started from the CCFM formalism [17–20], which explicitly involves two separate scales: the probing scale Q and the transverse momentum of the parton, $k_\perp$. The CCFM equations were subsequently extended to include the quarks, as well as reduced to the single-loop approximation. In addition, the non-Sudakov form factor was dropped. Kwieciński found that in this approximation the equations diagonalize in the space Fourier-conjugated to the transverse momentum, where they assume a particularly simple and elegant form in a close resemblance to the Dokshitzer-Gribov-Lipatov-Altarelli-Parisi (DGLAP) [37–40] equations for the integrated PDs. The only, but most important, difference is the appearance of the Bessel function $J_0(Qb)$ in the evolution kernel. Thus, the evolution depends on the transverse coordinate b. In the original work of Ref. [16] these equations were called ''the CCFM equations for the UPDs in the transverse-coordinate

*Electronic address: earriola@ugr.es
†Electronic address: Wojciech.Broniowski@ifj.edu.pl

space in the single-loop approximation.'' As a result of numerous steps leading away from the original CCFM, we find it more appropriate to call the equations of Ref. [16] *the Kwieciński equations for the UPD evolution*. Since in the case of integrated PDs these equations reduce to the usual leading-order (LO) DGLAP equations, the range of applicability of the Kwieciński equations is not larger as for the LO DGLAP equations, with not too small and not too large values of the Bjorken x variable.

Formally, the Kwieciński equations are integro-differential equations with the kernel depending on the transverse coordinate b (cf. Sec. II). As such, they are not trivial to solve numerically. The method of the original works [14–16] involved the Chebyshev interpolation in the x and Q spaces for each value of b. In this paper we offer an alternative method, based on the evolution of the x moments of UPDs. In the moment (Mellin) space, the evolution equations become a set of ordinary differential equations, which can be solved numerically in a very efficient way (see Sec. III). We derive analytic expressions for the b-dependent anomalous dimensions, which can be written in terms of hypergeometric functions. Then, the inverse Mellin transform to the original x space is performed via numerical integration with oscillatory functions. We show that the procedure is fast and stable, providing a useful numerical tool for evolving the UPDs.

The Mellin-transform method allows us to carry out analytic considerations, such as studies of certain limits of the equations, specifically the cases of low and large b, and x approaching the end points. We pursue these considerations, which can be done since the form of the b-dependent anomalous dimensions is analytic.

In addition to developing a different numerical method (Sec. III), our study differs from Ref. [16] in two physical aspects. First, rather than guessing the initial shape in b, we use the results of low-energy chiral quark models (Sec. IV). We consider two models: the recently proposed spectral quark model of Refs. [41–43] and the Nambu–Jona-Lasinio model with Pauli-Villars regularization [44]. These models were used before to describe the integrated PD [45–48] and were shown to do a surprisingly good job, in particular for the valence distribution in the pion. They were also used to describe successfully other aspect of high-energy processes, such as the pion distribution amplitude [49] and generalized (off-forward) PD of the pion [50,51]. The models give the initial condition at the model scale Q_0 in a particularly simple, factorized form. The valence quarks are distributed uniformly in x, while the gluons and sea quarks vanish. The b dependence is a simple, analytic function with exponential falloff at large b. We stress that the b dependence is a prediction of the model, rather than a mere guess, as is frequently made. Second, our implementation of the evolution switches from three to four flavors above the charm-production threshold, customarily taken at $Q^2=4\ \mathrm{GeV}^2$. Our numerical results are presented in Sec. V, where we show the dependence of the UPDs on x and b.

Since the analytic forms of the anomalous dimensions involve generalized hypergeometric functions, which may be cumbersome to program, we have developed a low-b expansion (Sec. VI), which makes the calculations simpler when b is not too large. The expansion is in powers of $b\Lambda_{\mathrm{QCD}}$, and is fast and stable. For the opposite problem, where Qb is large, we have obtained asymptotic expansions (Sec. VII), which allow us to deal numerically with the generalized hypergeometric functions.

Our method of solving the equations in Mellin space carries additional bonuses. In particular, it allows for analytic considerations in the investigation of formal limits at $x\to 1$ (Sec. VIII) and $x\to 0$ (Sec. IX). At $x\to 1$ we show that the b-dependent nonsinglet distribution approaches very fast the integrated nonsinglet distribution. At $x\to 0$ we find generalizations of the double-leading-logarithm (DLLA) formulas of Ref. [52]. Finally, we examine the large-b behavior, where we show that the evolution-generated UPDs from the Kwieciński equations exhibit power-law behavior at large b. The falloff is much faster for the gluons than for the quarks.

Widening in the transverse momentum of all partonic distributions is confirmed. We show that $\langle k_\perp^2\rangle$ grows with probing scale as $Q^2\alpha(Q^2)$. We write an approximating formula for the width for each partonic species, which may be useful in practical applications with the pion (Sec. X). The widening effect becomes stronger and stronger as Q increases or x decreases, and it is bigger for the gluons than for the nonsinglet and singlet quarks (see Sec. X).

The numerical method of this paper, which is easy to program and numerically fast and efficient, can be used for other initial conditions as well—for instance, for the Glück-Reya-Schienbein (GRS) [53] parametrization of the pion or the Glück-Reya-Vogt (GRV) parametrization [54], of the nucleon, supplied with a profile in the transverse coordinate, as originally studied in Ref. [16]. The only difference is in the form of the initial Mellin moments, which acquire a dependence on b. General predictions of the method in formal limits are listed in Sec. XI.

The appendixes contain many technical details, such as the perturbative QCD parameters and splitting functions (Appendix A), the analytic form of the b-dependent anomalous dimensions which enter the evolution in Mellin space (Appendix B), and their low-b (Appendix C) and high-b (Appendix D) expansion, as well as the pole-residue expansion (Appendix E). The latter is useful in analytic considerations near $x=0$.

II. KWIECIŃSKI EQUATIONS

In his studies of the UPDs, Kwieciński [14–16,22] started from the CCFM formalism [17–20] explicitly involving two separate scales: the probing scale Q and the transverse momentum of the parton, $k_\perp$. Then, the original CCFM equations were supplemented with quarks, as well as reduced to the single-loop approximation. The latter approximation replaces the angular ordering of the emitted gluons with the ordering of their transverse momenta. In addition, the non-Sudakov form factor was dropped. Kwieciński realized that the evolution equations for the UPDs acquire a particularly simple form in the transverse-coordinate space, b, conjugated to the transverse momentum $k_\perp$. For each distribution one introduces

$$f_j(x,b,Q)=\int_0^\infty 2\pi dk_\perp k_\perp J_0(bk_\perp) f_j(x,k_\perp,Q), \quad (2.1)$$

where $j=NS$ (nonsinglet quarks), S (singlet quarks), or G (gluons), and J_0 is the Bessel function. In order to avoid confusion, we stress that the transverse coordinate b, conjugated to the parton's transverse momentum, is not the impact parameter, appearing in the analysis of the generalized PDs. The latter quantity is conjugated to the transverse momentum transfer in off-forward scattering processes.

At $b=0$ the functions f_j are related to the integrated parton distributions $p_j(x,Q)$ as follows:

$$f_j(x,0,Q)=\frac{x}{2}p_j(x,Q). \quad (2.2)$$

More explicitly, for the case of the pion studied in this paper (we take π^+ for definiteness) we have

$$\begin{aligned} p_{\rm NS}&=\bar{u}-u+d-\bar{d},\\ p_S&=\bar{u}+u+d+\bar{d}+\bar{s}+s+\cdots,\\ p_{\rm sea}&\equiv p_S-p_{\rm NS}=2\bar{d}+2u+\bar{s}+s+\cdots,\\ p_G&=g, \end{aligned} \quad (2.3)$$

where the ellipses stand for higher flavors.

The Kwieciński equations read [16]

$$\begin{aligned} Q^2\frac{\partial f_{\rm NS}(x,b,Q)}{\partial Q^2}&=\frac{\alpha_s(Q^2)}{2\pi}\int_0^1 dz P_{qq}(z)\Big[\Theta(z-x)\\ &\times J_0((1-z)Qb) f_{\rm NS}\Big(\frac{x}{z},b,Q\Big)-f_{\rm NS}(x,b,Q)\Big], \end{aligned}$$

$$\begin{aligned} Q^2\frac{\partial f_S(x,b,Q)}{\partial Q^2}&=\frac{\alpha_s(Q^2)}{2\pi}\int_0^1 dz\Big\{\Theta(z-x)J_0((1-z)Qb)\\ &\times\Big[P_{qq}(z)f_S\Big(\frac{x}{z},b,Q\Big)+P_{qG}(z)f_G\Big(\frac{x}{z},b,Q\Big)\Big]\\ &-[zP_{qq}(z)+zP_{Gq}(z)]f_S(x,b,Q)\Big\}, \end{aligned}$$

$$\begin{aligned} Q^2\frac{\partial f_G(x,b,Q)}{\partial Q^2}&=\frac{\alpha_s(Q^2)}{2\pi}\int_0^1 dz\Big\{\Theta(z-x)J_0((1-z)Qb)\\ &\times\Big[P_{Gq}(z)f_S\Big(\frac{x}{z},b,Q\Big)+P_{GG}(z)f_G\Big(\frac{x}{z},b,Q\Big)\Big]\\ &-[zP_{GG}(z)+zP_{qG}(z)]f_G(x,b,Q)\Big\}. \end{aligned} \quad (2.4)$$

The splitting functions $P_{ab}(z)$ are listed in Eq. (A8).

Following Ref. [16], a factorized form of the distribution functions at the initial scale Q_0 is assumed,

$$f_j(x,b,Q_0)=F^{\rm NP}(b)\frac{x}{2}p_j(x,Q_0), \quad (2.5)$$

with the profile function $F^{\rm NP}(b)$ taken to be universal for all species of partons. The factorization assumption (2.5) is technical and one can easily depart from this limitation in numerical studies. We note, however, that the models of Refs. [42,44], studied in Sec. IV, do predict a factorized initial condition of the form (2.5). The input profile function $F^{\rm NP}(b)$ is linked through the Fourier-Bessel transform to the $k_\perp$ distribution at the scale Q_0. At $b=0$ the normalization is $F^{\rm NP}(0)=1$. The profile function factorizes from the evolution equations. This is clear, since any solution of Eq. (2.4) remains a solution when multiplied by an arbitrary function of b. As a result of evolution, at higher scales Q we have

$$f_j(x,b,Q)=F^{\rm NP}(b)f_j^{\rm evol}(x,b,Q), \quad (2.6)$$

with $f_j^{\rm evol}(x,b,Q)$ satisfying equations *identical* to Eq. (2.4).

We should stress again an important physical difference between $F^{\rm NP}(b)$ and $f_j^{\rm evol}(x,b,Q)$. While $F^{\rm NP}(b)$ originates entirely from low-energy, *nonperturbative* physics, $f_j^{\rm evol}(x,b,Q)$ is given by the *perturbative QCD evolution* with Eq. (2.4) from the initial condition

$$f_j^{\rm evol}(x,b,Q_0)=\frac{x}{2}p_j(x,Q_0). \quad (2.7)$$

Throughout this paper, except for Sec. IV, we focus on the perturbative evolution and the functions $f_j^{\rm evol}(x,b,Q)$. The function $F^{\rm NP}(b)$ is referred to as the *initial profile* and $f_j^{\rm evol}(x,b,Q)$ as the *evolution-generated UPD*.

III. KWIECIŃSKI EQUATION IN MELLIN SPACE

We define the x moments of an unintegrated parton distribution in impact parameter space as (we retain the same symbol for the function and its Mellin transform, hoping the distinction made by the argument prevents any confusion)

$$f_j(n,b,Q)=\int_0^1 dx x^{n-1}f_j(x,b,Q). \quad (3.1)$$

In Mellin space, the evolution equations for the UPDs are very simple, as they become diagonal in both b and n. They involve b-dependent anomalous dimensions, equal to

$$\gamma_{n,ab}(Qb) = 4\int_0^1 dz[z^n J_0((1-z)Qb)-1]P_{ab}(z) = \gamma^{(0)}_{n,ab} - 4\int_0^1 dz z^n[J_0((1-z)Qb)-1]P_{ab}(z), \tag{3.2}$$

where the values at $b=0$ are

$$\gamma^{(0)}_{n,NS} = -4\int_0^1 dz(z^n-1)P_{qq}(z),$$

$$\gamma^{(0)}_{n,qq} = -4\int_0^1 dz[(z^n-z)P_{qq} - zP_{Gq}],$$

$$\gamma^{(0)}_{n,qG} = -4\int_0^1 dz z^n P_{qG},$$

$$\gamma^{(0)}_{n,Gq} = -4\int_0^1 dz z^n P_{Gq},$$

$$\gamma^{(0)}_{n,GG} = -4\int_0^1 dz[(z^n-z)P_{GG} - zP_{qG}]. \tag{3.3}$$

Their explicit forms for various channels are listed in Eqs. (B6), (B7). The fact that we can write the analytic form of the integrals in Eq. (3.2) (see Appendix B) allows for efficient numerical calculations and analytic considerations.

The integration of both sides of Eq. (2.4) with $\int_0^1 dx x^{n-1}$ yields for the nonsinglet case the equation

$$\frac{df_{\rm NS}(n,b,Q)}{dQ^2} = -\frac{\alpha_S(Q^2)}{8\pi Q^2}\gamma_{n,NS}(Qb) f_{\rm NS}(n,b,Q). \tag{3.4}$$

The formal solution of Eq. (3.4) can be readily obtained as

$$\frac{f_{\rm NS}(n,b,Q)}{f_{\rm NS}(n,b,Q_0)} = \exp\left[-\int_{Q_0^2}^{Q^2}\frac{dQ'^2\alpha(Q'^2)}{8\pi Q'^2}\gamma_{\rm NS}(n,b,Q')\right]. \tag{3.5}$$

In the singlet channel we find the coupled set of equations

$$\frac{df_S(n,b,Q)}{dQ^2} = -\frac{\alpha_S(Q^2)}{8\pi Q^2}[\gamma_{n,qq}(Qb)f_S(n,b,Q) + \gamma_{n,qG}(Qb)f_G(n,b,Q)],$$

$$\frac{df_G(n,b,Q)}{dQ^2} = -\frac{\alpha_S(Q^2)}{8\pi Q^2}[\gamma_{n,Gq}(Qb)f_S(n,b,Q) + \gamma_{n,GG}(Qb)f_G(n,b,Q)], \tag{3.6}$$

which has the formal solution

$$\begin{pmatrix} f_S(n,b,Q) \\ f_G(n,b,Q)\end{pmatrix} = \mathcal{P}\exp\left[-\int_{Q_0^2}^{Q^2}\frac{dQ'^2\alpha(Q'^2)}{8\pi Q'^2}\Gamma_n(Qb)\right] \times \begin{pmatrix} f_S(n,b,Q_0) \\ f_G(n,b,Q_0)\end{pmatrix},$$

$$\Gamma_n(Qb) = \begin{pmatrix} \gamma_{n,qq}(Qb) & \gamma_{n,qG}(Qb) \\ \gamma_{n,Gq}(Qb) & \gamma_{n,GG}(Qb)\end{pmatrix}. \tag{3.7}$$

The symbol $\mathcal{P}$ indicates that powers of Γ_n are ordered along the integration path. The qualitative difference between Eq. (3.7) and the LO DGLAP equations is the fact that Γ_n depends on the evolution variable Q. This makes the singlet sector more difficult to analyze analytically. Equations (3.6) can be solved numerically for any value of n real or complex [55]. For the case of integrated PD ($b=0$) Eqs. (3.4) and (3.6) reduce to the well-known LO DGLAP equation in Mellin space.

The corresponding UPD in x space can be reconstructed using the inverse Mellin transform

$$f_j(x,b,Q) = \int_{n_0-i\infty}^{n_0+i\infty}\frac{{\rm d}n}{2\pi i}x^{-n}f_j(n,b,Q), \tag{3.8}$$

where n_0 has to be chosen in such a way as to leave all the singularities on the left-hand side of the contour. It turns out that for $b\neq 0$ the analytic structure of the b-dependent anomalous dimension remains the same as for the $b=0$ case. This can be inferred directly by studying the analytic structure of the formulas (B6), (B7) or the pole-residue expansion of Eq. (E4). Thus, we have the result that $\gamma_{n,NS}(Qb)$, $\gamma_{n,qq}(Qb)$, and $\gamma_{n,qG}(Qb)$ have poles at $n=-1,-2,-3,\ldots$, while $\gamma_{n,GG}(Qb)$ and $\gamma_{n,Gq}(Qb)$ have poles at $n=0,-1,-2,\ldots$. Parametrizing the contour in Eq. (3.8) as $n=n_0+it$, we arrive at the inversion formula

$$f_j(x,b,Q) = x^{-n_0}\int_0^\infty\frac{{\rm d}t}{\pi}\{\cos(t\log x){\rm Re}[f_j(n_0+it,b,Q)] + \sin(t\log x){\rm Im}[f_j(n_0+it,b,Q)]\}. \tag{3.9}$$

For the nonsinglet case we take $n_0=0$, while for the singlet case $n_0=1$. As an additional check we have also verified that a bended integration path $n=c+re^{i\pi/4}$ with $0\leqslant r<\infty$, as used in [55], also works nicely.

IV. INITIAL CONDITION FOR THE UPD OF THE PION

As an illustration of our method, we consider the UPDs of the pion with the initial condition at Q_0 provided by two large-N_c low-energy chiral quark models. The original work of Ref. [16] tested the GRS parametrization for the pion [53] and the GRV parametrization for the nucleon [54], supplied with a Gaussian profile $F^{\rm NP}(b)$. The considered models generate the functions $F^{\rm NP}(b)$ as genuine model predictions of low-energy nonperturbative physics, with no freedom involved. Our first model is the recently proposed spectral

quark model (SQM) [41–43], and the second one is the popular Nambu–Jona Lasinio model (NJL) with Pauli-Villars (PV) regularization [44], treated for simplicity in the strict chiral limit.

First, since the chiral quark models have no gluon degrees of freedom, we have, at the model scale,

$$g(x,Q_0)=0 \tag{4.1}$$

or

$$f_G^{\rm evol}(x,b,Q_0)=0. \tag{4.2}$$

For the integrated valence quark PD both models predict, in the chiral limit and at the model scale Q_0, that

$$q(x,Q_0)=\theta(x)\,\theta(1-x), \tag{4.3}$$

i.e., a constant value with the proper normalization and support. Thus the corresponding $f^{\rm evol}$ functions of Eq. (2.2) are linear in x:

$$f_{NS,S}^{\rm eol}(x,b,Q_0)=x\,\theta(x)\,\theta(1-x). \tag{4.4}$$

The scale of the model, as found from the momentum sum rule, is rather low: $Q_0=313$ MeV. Although this is admittedly a very low scale, one may hope that the typical expansion parameter $\alpha(Q_0^2)/(2\pi)\sim 0.3$ is low enough to make the perturbation theory sensible. This claim gains support from the next-to-leading analysis of the integrated PDs [45], where the corrections are found to be small. The initial conditions provided by the chiral quark models, where only the valence quarks are present, work well for the nonsinglet quarks. On the other hand, in the singlet channel they lead to an underestimation of gluons at large x and too steep gluon distributions at low x [56,57]. Hence, in the singlet channel other initial conditions should be used.

The QCD evolution is crucial for the phenomenological success of the considered low-energy chiral quark models. In Refs. [45–47] it has been found that the nonsinglet distribution, when evolved to the scale of 2 GeV, agrees very well with the Sutton-Martin-Roberts-Sterling (SMRS) parametrization of the pion data [58], while in [59] it has been very favorably compared to the old E615 data at 4 GeV [60] (see the discussion in Sec. V and Fig. 5).

In the SQM, the valence UPD of the pion at the scale Q_0 is [42]

$$q(x,k_\perp,Q_0)=\overline{q}(1-x,k_\perp)$$

$$=\frac{6M_V^3}{\pi(k_\perp^2+M_V^2/4)^{5/2}}\,\theta(x)\,\theta(1-x), \tag{4.5}$$

where $M_V=770$ MeV is the mass of the ρ meson. Passing to impact-parameter space with the Fourier-Bessel transform yields

$$q(x,b,Q_0)\equiv 2\pi\int_0^\infty k_\perp dk_\perp\, q(x,k_\perp)J_0(k_\perp b)$$

$$=\left(1+\frac{bM_V}{2}\right)\exp\left(-\frac{M_V b}{2}\right)\theta(x)\,\theta(1-x). \tag{4.6}$$

The expansion at small b gives

$$q(x,b,Q_0)=\left(1-\frac{M_V^2b^2}{8}+\frac{M_V^3b^3}{24}+\cdots\right)\theta(x)\,\theta(1-x), \tag{4.7}$$

and average transverse momentum squared is equal to

$$\langle k_\perp^2\rangle_{\rm NP}^{\rm SQM}\equiv\frac{\int d^2k_\perp k_\perp^2 q(x,k_\perp)}{\int d^2k_\perp q(x,k_\perp)}=-\frac{4}{q(x,b)}\frac{dq(x,b)}{db^2}\bigg|_{b=0}$$

$$=\frac{M_V^2}{2}, \tag{4.8}$$

which numerically gives $\langle k_\perp^2\rangle_{\rm NP}^{\rm SQM}=(544\ {\rm MeV})^2$ (all at the model working scale Q_0). The subscript *NP* reminds us that the quantity comes entirely from the nonperturbative physics, entering the profile function $F^{\rm NP}(b)$ (see the discussion at the end of Sec. II).

In the NJL model with PV regularization [44] the analogous formulas read [48]

$$q(x,k_\perp,Q_0)=\overline{q}(1-x,k_\perp)$$

$$=\frac{\Lambda^4M^2N_c}{4f_\pi^2\pi^3(k_\perp^2+M^2)(k_\perp^2+\Lambda^2+M^2)^2}$$

$$\times\theta(x)\,\theta(1-x), \tag{4.9}$$

$$q(x,b,Q_0)=\frac{M^2N_c}{4f_\pi^2\pi^2}\left(2K_0(bM)-2K_0(b\sqrt{\Lambda^2+M^2})\right.$$

$$\left.-\frac{b\Lambda^2K_1(b\sqrt{\Lambda^2+M^2})}{\sqrt{\Lambda^2+M^2}}\right)\theta(x)\,\theta(1-x), \tag{4.10}$$

where the pion decay constant is given by

$$f_\pi^2=\frac{M^2N_c\left(\Lambda^2+(\Lambda^2+M^2)\log\frac{\Lambda^2+M^2}{M^2}\right)}{4\pi^2(\Lambda^2+M^2)}. \tag{4.11}$$

The parameters of the model are adjusted in such a way that $f_\pi=93$ MeV—namely, $M=280$ MeV and $\Lambda=871$ MeV. The expansion at small b yields

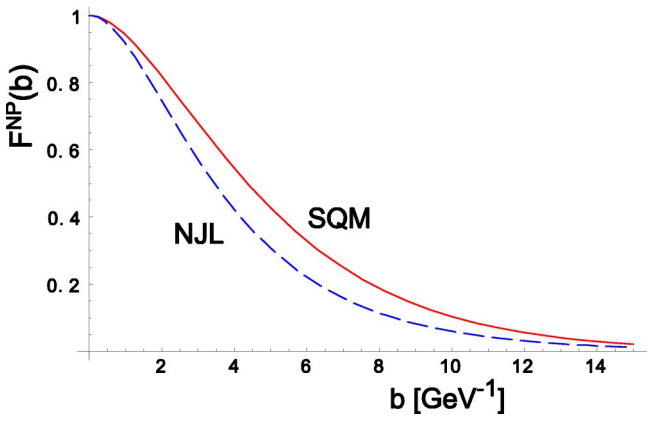

FIG. 1. The initial profile functions $F_{\rm NP}$ for the SQM and NJL models, plotted as functions of the transverse coordinate b. The falloff is exponential, according to Eqs. (4.14) and (4.10).

$$q(x,b,Q_0)=\left(1-\frac{M^2N_c\left(\Lambda^2-M^2\log\frac{\Lambda^2+M^2}{M^2}\right)b^2}{16\pi^2f_\pi^2}+\cdots\right)\theta(x)\,\theta(1-x), \tag{4.12}$$

and the average transverse momentum squared is equal to

$$\langle k_\perp^2\rangle_{\rm NP}^{\rm NJL}=\frac{M^2N_c\left(\Lambda^2-M^2\log\frac{\Lambda^2+M^2}{M^2}\right)}{4\pi^2f_\pi^2}, \tag{4.13}$$

which numerically gives $\langle k_\perp^2\rangle_{\rm NP}^{NJL}=(626\ {\rm MeV})^2$ (at the scale Q_0), which is similar to the number from the SQM.

Finally, in the notation of Eq. (2.6) we can write that the initial profile function is

$$F_{\rm SQM}^{\rm NP}(b)=\left(1+\frac{bM_V}{2}\right)\exp\left(-\frac{M_Vb}{2}\right), \tag{4.14}$$

$$F_{\rm NJL}^{\rm NP}(b)=\frac{M^2N_c}{4f_\pi^2\pi^2}\left(2K_0(bM)-2K_0(b\sqrt{\Lambda^2+M^2})-\frac{b\Lambda^2K_1(b\sqrt{\Lambda^2+M^2})}{\sqrt{\Lambda^2+M^2}}\right). \tag{4.15}$$

Both initial profile functions are displayed in Fig. 1. Note that the profiles, although having a b^2 correction at small b, are not Gaussian and at large b display an exponential falloff.

As discussed in Sec. II, the form of $F^{\rm NP}(b)$ factorizes from the evolution. In both models there is no dependence of the UPDs on x at the initial scale Q_0. As a result, we get the following set of initial moments:

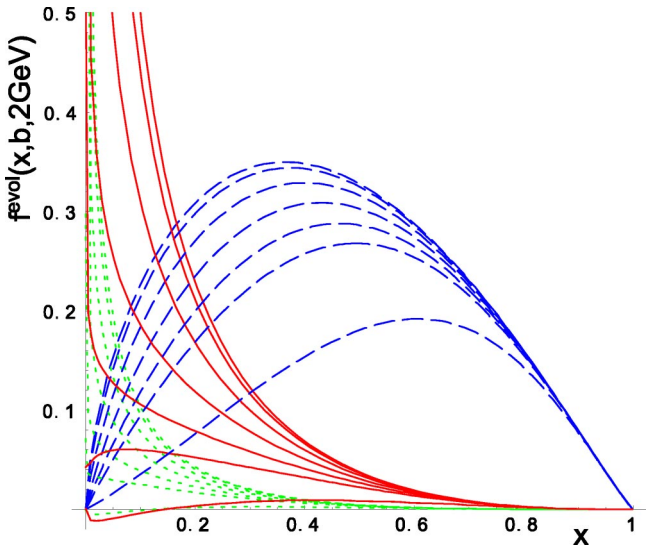

FIG. 2. The evolution-generated UPDs for the pion for various values of the transverse coordinate (from top to bottom $b=0$, 1, 2, 3, 4, 5, and 10 GeV^{-1}), plotted as functions of the Bjorken x. The evolution is made with the initial condition (4.4) at $Q_0=313$ MeV up to $Q=2$ GeV. Solid lines: gluons. Dashed lines: valence quarks. Dotted lines: sea quarks.

$$f_{\rm NS}^{\rm evol}(n,b,Q_0)=\frac{1}{n+1},$$

$$f_S^{\rm evol}(n,b,Q_0)=\frac{1}{n+1},$$

$$f_G^{\rm evol}(n,b,Q_0)=0. \tag{4.16}$$

We remark that away from the chiral limit the separability of the dependence on x and b no longer holds. In this case the initial conditions for the evolution are more complicated (they depend on b), but the analysis can be easily generalized to account for this case as well.

V. NUMERICAL RESULTS

In Fig. 2 we present the results of our numerical calculation with the method using the Mellin transform. The initial conditions are for the pion in the chiral limit (4.16), holding at $Q_0=313$ MeV, and the evolution is carried up to the scale of $Q=2$ GeV. The differential equations for the moments, Eqs. (3.4), (3.6), are solved numerically for complex n values along the Mellin contour, and subsequently the inverse Mellin transform (3.9) is carried out. The figure contains three families of curves, solid for the gluon, dashed for the valence quarks, and dotted for the sea quarks. In each family b assumes the values 0, 1, 2, 3, 4, 5, and 10. Naturally, increasing b results in a decrease of the distribution, with the effect strongest at low x. At x close to 1 this effect disappears, which is explained in Sec. VIII. We also note that at high values of b the distributions for the gluons become negative, reflecting the change of sign of the Bessel function in the evolution kernel of Eq. (2.4). As already discussed in Ref. [16], this poses no immediate physical problems, as the

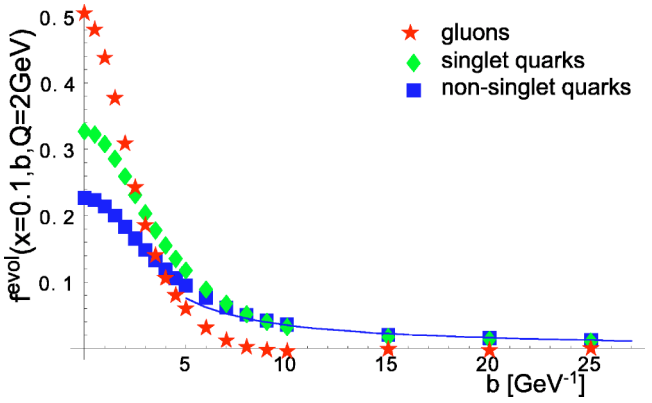

FIG. 3. Evolution-generated UPDs for the pion for $Q=2$ GeV and $x=0.1$, plotted as functions of b. The evolution is made with the initial condition (4.4) at $Q_0=313$ MeV. The numerical results are represented by squares for the nonsinglet quarks, diamonds for the singlet quarks, and stars for the gluons, while the solid line shows the asymptotic formula (7.5) for the case of nonsinglet quarks. We note the much faster falloff for the gluons than for the quarks, as expected from Eq. (7.8). The quarks exhibit a long-range tail, according to the power-law formula (7.5). As Q is increased or x decreased, the distributions in b become narrower, leading to spreading in $k_\perp$.

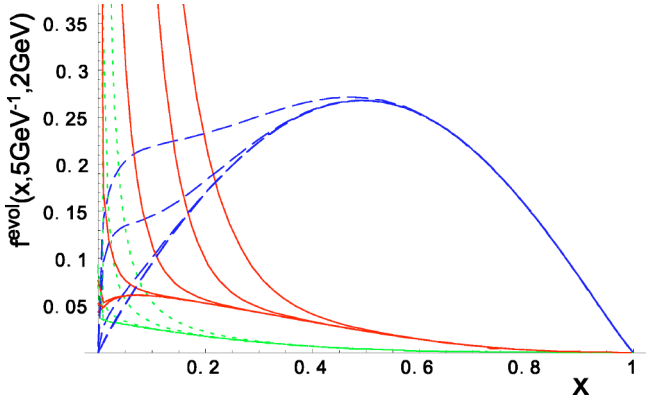

FIG. 4. The low-b expansion for the evolution-generated UPDs of the pion at $b=5$ GeV^{-1} and $Q=2$ GeV^2, plotted as a function of the Bjorken x. Solid lines: gluons. Dashed lines: valence quarks. Dotted lines: sea quarks. For each kind of parton the curves from top to bottom correspond to 2, 4, 6, 8, 10, and 16 terms in the small-b expansion. The initial condition for the evolution is provided by Eq. (4.4).

distributions in $k_\perp$ remain positive as primary objects and so are the physical cross sections.

The results of Fig. 2 are consistent with the findings of Ref. [16], where a different numerical method was used, as well as a different initial condition tested.

In Fig. 3 we show the dependence of the evolution-generated UPDs on b at $Q=2$ GeV and $x=0.1$. The results are represented by squares for the nonsinglet quarks, diamonds for the singlet quarks, and stars for the gluons. We note the much faster falloff with b for the gluons than for the quarks, as expected from Eq. (7.8). The quarks exhibit a long-range tail, according to the power-law formula (7.5). The solid line shows the asymptotic form for the case of nonsinglet quarks from Eqs. (7.5), (7.6) (see Sec. VII), which becomes accurate for $b \geqslant 10$ GeV^{-1}. As Q is increased further or x decreased, the distributions in b become narrower, leading to larger spreading in $k_\perp$. For more details and plots concerning other numerical results see Ref. [16].

The curve for the gluon at $b=10$ GeV^2 turns negative at low x. The same phenomenon was found in Ref. [16] with a different initial condition. To our knowledge, this does not lead to any physical problems. The issue lies in taking the Fourier-Bessel transform of Eq. (2.1). The UPDs in the $k_\perp$ representations are positive [16] and so are the physical quantities computed with the UPDs in the momentum representation. However, a Fourier-Bessel transform of a positive-definite function need not be positive definite. This is the case of the gluon in Fig. 2 for certain sufficiently large values of b.

VI. LOW-b EXPANSION

Since the anomalous dimensions (B6), (B7) involve generalized hypergeometric functions, they are not easy to use in numerical calculations. For that reason we consider the small-b expansion, as well as the asymptotic forms at large bQ, presented in the next section. It is convenient to introduce the notation

$$r_k = r_k(Q_0^2, Q^2) = \int_{Q_0^2}^{Q^2} \frac{dQ'^2 \alpha(Q'^2)}{8\pi Q'^2} Q'^{2k}. \qquad (6.1)$$

The explicit form of functions r_k is given in Appendix A. Next, we apply Eq. (C4) and find the following expansion in the nonsinglet channel:

$$\frac{f(n,b,Q)}{f(n,b,Q_0)} = e^{\gamma^{(0)}_{n,NS} r_0} \exp\left[-C_F \sum_{k=1}^{\infty} \frac{(-b^2)^k 4^{1-k}}{k!^2} \times [\mathrm{B}(2k, n+1) + \mathrm{B}(2k, n+3)] r_k \right], \qquad (6.2)$$

where B is the Euler beta function. We note that although at the level of the differential equation our expansion is formally in Qb, the result (6.2), together with the fact that r_k is proportional to $\Lambda_{\mathrm{QCD}}^{2k}$ [cf. Eq. (A4)], shows that the expansion parameter is actually $b\Lambda_{\mathrm{QCD}}$. The rate of convergence of the method can be deduced from Fig. 4. As we can see, the number of terms needed increases for increasing b and decreasing x. For $x>0.01$ eight terms in the expansion seem more than sufficient.

VII. LARGE-b EXPANSION

Appendix D contains asymptotic forms of the generalized hypergeometric functions and of the b-dependent anomalous dimensions. These expressions hold in the limit of large Qb at n kept fixed. The formulas are of great practical importance in the present study, since they are much simpler to implement in numerical calculations than the generalized hypergeometric functions appearing in Eqs. (B6), (B7). Actu-

ally, Eqs. (D3)–(D6) should be used whenever Qb is larger than about $10|n|$. Since in practical problems the scale Q may be as large as the mass of the W boson, there is a frequent need to use the asymptotic expressions (D3)–(D6). Also, if the UPDs in the transverse momentum are needed, one has to carry back the Fourier transform from b space to $k_\perp$ space, which involves all values of b.

We start with the nonsinglet case of Eq. (3.4). With the help of Eq. (D3), where at the leading order in $1/(Qb)$ we drop the oscillatory parts, we may write Eq. (3.5) at large Qb:

$$\frac{f_{\rm NS}^{\rm evol}(n,b,Q)}{f_{\rm NS}^{\rm evol}(n,b,Q_0)} = e^{y_0+y_1 n}, \tag{7.1}$$

where

$$y_1 = -4C_F\left(\frac{2\Lambda_{\rm QCD}^2}{b} - \frac{1}{b^3}\right) r_{-3/2}(Q_0^2,Q^2),$$

$$y_0 = -4C_F\left(\frac{2\Lambda_{\rm QCD}^2}{b} r_{-3/2}(Q_0^2,Q^2) + \frac{1}{\beta_0^{(3)}}\log\frac{Q}{Q_0} + 2\left[\log\frac{b\Lambda_{\rm QCD}}{2} + \gamma - \frac{3}{4}\right] r_0(Q_0^2,Q^2)\right),$$

$$\text{for } Q^2 < \mu_c^2, \tag{7.2}$$

and

$$y_1 = -4C_F\left(\frac{2\Lambda_{\rm QCD}^2}{b} r_{-3/2}(Q_0^2,\mu_c^2) + \frac{2\Lambda_4^2}{b} r_{-3/2}(\mu_c^2,Q^2) - \frac{1}{b^3} r_{-3/2}(Q_0^2,Q^2)\right),$$

$$y_0 = -4C_F\left(\frac{2\Lambda_{\rm QCD}^2}{b} r_{-3/2}(Q_0^2,\mu_c^2) + \frac{2\Lambda_4^2}{b} r_{-3/2}(\mu_c^2,Q^2) + \frac{1}{\beta_0^{(3)}}\log\frac{\mu_c}{Q_0} + \frac{1}{\beta_0^{(4)}}\log\frac{Q}{\mu_c} + 2\left[\log\frac{b\Lambda_{\rm QCD}}{2}\right] r_0(Q_0^2,\mu_c^2) + 2\left[\log\frac{b\Lambda_4}{2}\right] r_0(\mu_c^2,Q^2) + \left[\gamma - \frac{3}{4}\right] r_0(Q_0^2,Q^2)\right),$$

$$\text{for } Q^2 \geqslant \mu_c^2. \tag{7.3}$$

Next, we take our initial condition (4.16) and use the inverse Mellin transform

$$\int_C \frac{dn}{2\pi i} x^{-n} \frac{e^{y_0+y_1 n}}{n+1} = x e^{y_0 - y_1}\Theta\left(y_1 + \log\frac{1}{x}\right). \tag{7.4}$$

The condition provided by the theta function means that the formula can be used for $x < \exp(y_1)$. For negative y_1 this means that the validity is limited for x not too close to 1. This, however, has been already tacitly assumed, since the asymptotic expansion holds for fixed values of n and hence cannot describe x in the vicinity of 1. The above formulas lead to the following large-b form of $f_{\rm NS}^{\rm evol}$ in x space:

$$f_{\rm NS}^{\rm evol}(x,b,Q) = x\left(\frac{b\Lambda_{\rm QCD}}{2}\right)^{-8C_F r_0(Q_0^2,Q^2)}\left(\frac{Q}{Q_0}\right)^{-4C_F/\beta_0^{(3)}} \times \exp\left(\left[2\gamma - \frac{3}{2}\right] r_0(Q_0^2,Q^2) + \frac{1}{b^3} r_{-3/2}(Q_0^2,Q^2)\right),$$

$$\text{for } Q^2 < \mu_c^2, \tag{7.5}$$

and

$$f_{\rm NS}^{\rm evol}(x,b,Q) = x\left(\frac{b}{2}\right)^{-8C_F r_0(Q_0^2,Q^2)} \Lambda_{\rm QCD}^{-8C_F r_0(Q_0^2,\mu_c^2)} \Lambda_4^{-8C_F r_0(\mu_c^2,Q^2)} \times \left(\frac{\mu_c}{Q_0}\right)^{-4C_F/\beta_0^{(3)}}\left(\frac{Q}{\mu_c}\right)^{-4C_F/\beta_0^{(4)}} \times \exp\left(\left[2\gamma - \frac{3}{2}\right] r_0(Q_0^2,Q^2) + \frac{1}{b^3} r_{-3/2}(Q_0^2,Q^2)\right),$$

$$\text{for } Q^2 \geqslant \mu_c^2. \tag{7.6}$$

We note a few facts: the nonsinglet UPD of the pion is for large Qb linear in x for x not too close to 1, with the slope decreasing with b as a power law [we can neglect here the small correction due to the last term in Eqs. (7.5), (7.6)]. The exponent of b is $-8C_F r_0(Q_0^2,Q^2)$. The overall constant is also determined. Note that linearity with x at not-too-large x is seen in Fig. 2 for the valence quarks (dashed lines) at $b = 10\ \text{GeV}^{-1}$. Numerically, at $Q = 2$ GeV we find for low x that $f_{\rm NS}(x, b = 5\ \text{GeV}^{-1}, Q = 2\ \text{GeV}) = 0.73x$ and $f_{\rm NS}(x, b = 10\ \text{GeV}^{-1}, Q = 2\ \text{GeV}) = 0.35x$, in accordance with the exact calculation of Fig. 2.

The asymptotic form (7.5), (7.6) works very efficiently in practice. For the case of the nonsinglet quarks this can be seen from Fig. 3, where for $Q = 2$ GeV and $b > 5\ \text{GeV}^{-1}$ there is virtually no difference between the exact numerical calculation and the asymptotic formula.

The power-law behavior in b shows that the evolution generates a rather weak behavior at large b. Numerically, at $Q = 2$, 4, and 100 GeV, the power of b is, respectively, -1.12, -1.29, and -1.75. This means that the large-b behavior for the nonsinglet quarks is controlled by the initial profile $F^{\rm NP}(b)$, which in chiral quark models of the pion has an exponential falloff, rather than by the QCD evolution.

Now we pass to the discussion of the singlet case of Eq. (3.6). In the large-Qb limit the leading part of the matrix Γ_n of Eq. (3.7) becomes

$$\Gamma_n(Qb)\to\begin{pmatrix} 4C_F\log\dfrac{Q^2b^2}{4} & 0 \\ 0 & 4N_c\log\dfrac{Q^2b^2}{4}\end{pmatrix}. \quad (7.7)$$

From this form, using methods as for the nonsinglet case above, we infer that the dependence on b, is asymptotically,

$$f_S(x,b,Q)\sim b^{-8C_Fr_0(Q_0^2,Q^2)},$$

$$f_G(x,b,Q)\sim b^{-8N_cr_0(Q_0^2,Q^2)}. \quad (7.8)$$

Thus the singlet quarks fall off at the same rate as the nonsinglet quarks of Eqs. (7.5), (7.6), while the gluons drop significantly faster, as $C_f=4/3$ and $N_c=3$. This behavior is clearly seen in Fig. 3. We note that due to the complications of Eq. (3.7) a more detailed analysis yielding prefactors, such as the one for the nonsinglet case presented above, is more difficult in the present case, and hence we do not pursue it further here.

We end this section with a couple of remarks concerning the observed long-range nature of the tails in b. Our initial nonperturbative profiles $F^{\rm NP}(b)$ drop exponentially and therefore suppress the tails generated by the evolution. This means that the large-b or low-$k_\perp$ behavior is controlled by nonperturbative effects. The larger negative power in f_G, Eq. (7.8), explains the faster shrinkage of gluon distributions in b space or faster spreading in $k_\perp$ space.

VIII. BEHAVIOR OF $F_{\rm NS}$ AT $x\to1$

According to standard properties of the Mellin transform, the limit $x\to1$ is obtained form the large-n behavior of the anomalous dimensions. Using the asymptotic form $B(n,m)\to\Gamma(m)/n^m$ in Eq. (C4) or the explicit form of the anomalous dimensions (B6), (B7), one obtains that

$$\gamma_{n,NS}(Qb)-\gamma^{(0)}_{n,NS}=2C_F\frac{b^2Q^2}{n^2}+\mathcal{O}(1/n^3). \quad (8.1)$$

We also need the large-n expansion of $\gamma^{(0)}_{n,NS}$, which is

$$\gamma^{(0)}_{n,NS}=8C_F[\log n+\gamma-3/4+R(n)], \quad (8.2)$$

where $R(n)=\Sigma_{k=1}^{\infty}c_kn^{-k}$. Thus, according to Eq. (3.5), we have the asymptotic form

$$\frac{f^{\rm evol}_{\rm NS}(n,b,Q^2)}{f^{\rm evol}_{\rm NS}(n,b,Q_0^2)}=n^{-8C_Fr_0(Q^2,Q_0^2)}e^{-8C_Fr_0[\gamma-3/4+R(n)]}\times e^{2C_Fb^2r_1/n^2+\mathcal{O}(1/n^3)}. \quad (8.3)$$

Using the initial moments (4.16) and expanding the exponentials in Eq. (8.3) we obtain

$$f^{\rm evol}_{\rm NS}(n,b,Q^2)=\frac{1}{n+1}n^{-8C_Fr_0}\left(1+\sum_{k=1}^{\infty}c_k'n^{-k}\right)\times[1+2C_Fb^2r_1/n^2+\mathcal{O}(1/n^3)]. \quad (8.4)$$

Next, we use the formula for the inverse Mellin transform,

$$\int_C dnx^{-n}\frac{n^{-A}}{n+w}=(-w)^{-A}x^w\left(1-\frac{\Gamma\left(A,-w\log\dfrac{1}{x}\right)}{\Gamma(A)}\right)\to\frac{x^w\left(\log\dfrac{1}{x}\right)^A}{A\Gamma(A)}, \quad (8.5)$$

which after a straightforward algebra leads to the equation

$$\frac{f^{\rm evol}_{\rm NS}(x,b,Q^2)}{f^{\rm evol}_{\rm NS}(x,0,Q^2)}=1-\frac{2C_Fb^2r_1(1-x)^2}{(1+8C_Fr_0)(2+8C_Fr_0)}+\mathcal{O}((1-x)^3). \quad (8.6)$$

The terms with coefficients c_k' do not enter at the leading order in $(1-x)$. The behavior of Eq. (8.6) agrees with the behavior of Fig. 2, where close to $x=1$ the departure of the curves with finite b from the curve with $b=0$ becomes very slow, as it is suppressed by $(1-x)^2$.

We also obtain that at $x\to1$ the integrated nonsinglet distribution behaves as

$$f_{\rm NS}(x,0,Q^2)\to\frac{e^{2C_F(3-4\gamma)r_0}}{\Gamma(1+8C_Fr_0)}(1-x)^{8C_Fr_0}. \quad (8.7)$$

This agrees with the fact that a function which originally behaves at $x\to1$ as $f_{\rm NS}(x,0,Q_0)\to(1-x)^p$ evolves into [61]

$$f_{\rm NS}(x,0,Q^2)\to(1-x)^{p-(4C_F/\beta_0)\log[\alpha(Q)/\alpha(Q_0)]}. \quad (8.8)$$

In our approach the integrated function at $Q=Q_0$ has $p=0$. Numerically, we find that

$$f_{\rm NS}(x,0,(2\ {\rm GeV})^2)\to1.15(1-x)^{1.13},$$

$$f_{\rm NS}(x,0,(4\ \ {\rm GeV})^2)\to1.08(1-x)^{1.29}. \quad (8.9)$$

Note that although with the DGLAP evolution the Brodsky-Lepage counting rules for the behavior at $x\to1$ are clearly disobeyed, our numerical predictions agree within experimental uncertainties with the experimental data, including the region very close to $x=1$. Figure 5 confronts our results evolved to the scale of $Q=4$ GeV to the E615 experimental Drell-Yan data [60] which cover the large-x region. In view of the simplicity of the present model, the quality of this comparison is impressive.

On the other hand, it is believed that at $x\to1$ it is necessary to resum the soft gluon processes, which leads to summing up powers of $\log(1-x)$. Clearly, such effects are not included in the considered evolution.

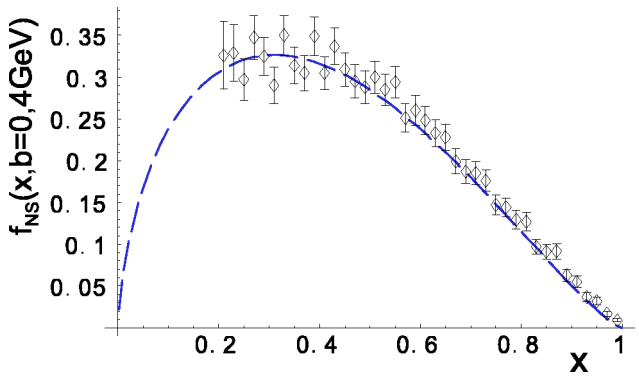

FIG. 5. Model prediction for the *integrated* valence quark distribution of the pion, evolved to from the initial condition (4.16) to the scale of $Q=4$ GeV, confronted with the E615 Drell-Yan data [60]. The behavior at $x\to 1$ is $(1-x)^{1.29}$.

IX. BEHAVIOR AT $x\to 0$

The results at $x\to 0$ are of formal rather than physical significance, since the considered evolution, being a generalization of LO DGLAP equations for UPDs, does not describe properly the physics at very small values of x. The low-x behavior of the inverse Mellin transform is encoded in the closest singularities to the integration line. We start with the nonsinglet case of Eq. (3.4). Using the pole-residue expansion of Appendix E we find that the closest singularity is at $n=-1$, with residue $-4C_F J_0(Qb)$. With the help of the expression for the inverse Mellin transform,

$$\int_{-i\infty}^{i\infty}\frac{dn}{2\pi i}\frac{x^{-n}}{n+1}e^{a/(n+1)}=\begin{cases} xI_0\left(2\sqrt{a\log\frac{1}{x}}\right), & a\geqslant 0,\\ xJ_0\left(2\sqrt{a\log\frac{1}{x}}\right), & a<0,\end{cases} \tag{9.1}$$

we find that

$$f_{\rm NS}^{\rm evol}(x,b,Q^2)\to\begin{cases} xI_0\left(2\sqrt{C_F A\log\frac{1}{x}}\right), & A\geqslant 0,\\ xJ_0\left(2\sqrt{C_F A\log\frac{1}{x}}\right), & A<0,\end{cases} \tag{9.2}$$

where

$$A=\int_{Q_0^2}^{Q^2}\frac{dQ^2}{2\pi Q^2}\alpha(Q^2)J_0(Qb). \tag{9.3}$$

For the singlet case we retain the closest singularity at $n=0$ and rewrite Eq. (3.7) in the form

$$\begin{pmatrix} f_S(n,b,Q)\\ f_G(n,b,Q)\end{pmatrix}=\exp\left[\int_{Q_0^2}^{Q^2}\frac{dQ'^2\alpha(Q'^2)J_0(Q'b)}{\pi Q'^2}\times\begin{pmatrix} 0 & 0\\ \frac{C_F}{n} & \frac{N_c}{n}\end{pmatrix}\right]\begin{pmatrix} f_S(n,b,Q_0)\\ f_G(n,b,Q_0)\end{pmatrix}, \tag{9.4}$$

where we have used Eq. (E6) and could drop the $\mathcal{P}$ symbol since in the present approximation the matrix in the exponent does not depend on Q'. After some straightforward algebra we obtain

$$f_S(n,b,Q)=f_S(n,b,Q_0),$$

$$f_G(n,b,Q)=f_S(n,b,Q_0)\frac{C_F}{N_c}(e^{2N_cA/n}-1)+f_G(n,b,Q_0)e^{2N_cA/n}. \tag{9.5}$$

The equation for f_S shows the inadequacy of retaining for this case the singularity at $n=0$ only, as in the considered limit of $x\to 0$ the singlet quarks are controlled by the singularity at $n=-1$. For the case of gluons we use the initial condition (4.16). We need the inverse Mellin transform

$$\int_C dn x^{-n}\frac{1}{n+1}\exp\left(\frac{a}{n}\right)=\sum_{k=0}^{\infty}(-1)^k\left(\frac{\log\frac{1}{x}}{a}\right)^{k/2}I_k\left(2\sqrt{a\log\frac{1}{x}}\right)\sim\frac{\exp\left(2\sqrt{a\log\frac{1}{x}}\right)}{\sqrt{4\pi\sqrt{a\log\frac{1}{x}}}\left(1+\sqrt{\frac{\log\frac{1}{x}}{a}}\right)},\quad a>0, \tag{9.6}$$

where in the last line we have used the asymptotic form of the Bessel functions. With this result we find that the unintegrated gluon distribution at $x\to 0$ behaves as

$$f_G(n,b,Q)\sim\exp\left(2\sqrt{2N_cA\log\frac{1}{x}}\right),\quad A>0, \tag{9.7}$$

with A provided in Eq. (9.3). If $a<0$ in Eq. (9.6), then the I_k functions above are replaced with the J_k functions, and the asymptotics changes the character from exponential to oscillatory:

$$f_G(n,b,Q)\sim\left[\left(1+\sqrt{\frac{\log\frac{1}{x}}{-A}}\right)\cos\left(2\sqrt{-A\log\frac{1}{x}}\right)+\left(1-\sqrt{\frac{\log\frac{1}{x}}{-A}}\right)\sin\left(2\sqrt{-A\log\frac{1}{x}}\right)\right]\times\frac{1}{\sqrt{\pi\sqrt{-A\log\frac{1}{x}}}\left(1-\frac{\log\frac{1}{x}}{A}\right)},$$

$$A<0. \tag{9.8}$$

For $b=0$ the result (9.7) is consistent with the DLLA for the DGLAP equation [52], where one obtains, with constant α,

$$xg(x,Q)\sim\exp\left(2\sqrt{\frac{N_c}{\pi}\alpha\log\frac{Q^2}{Q_0^2}\log\frac{1}{x}}\right). \tag{9.9}$$

See, e.g., the review in Ref. [62]. Our formulas (9.2) and (9.7) are generalizations of this behavior for the unintegrated distributions evolved with Eq. (2.4).

The pole-residue expansion of Appendix E is good for not-too-large Qb. This limitation, at any fixed x, carries over to Eq. (9.2) Numerically, we find that, at $x=0.1$, Eq. (9.2) is valid for $Qb\leqslant 5$. For higher values corrections from further residues should be included.

X. EVOLUTION OF $\langle k_\perp^2\rangle$

The average transverse momentum squared is a convenient measure of the width of the UPDs. As a result of the factorization of the initial profile, Eq. (2.6), $\langle k_\perp^2\rangle$ decomposes into two terms: the contribution from the initial profile $F^{\rm NP}$ gives the width at the initial scale $Q=Q_0$ and the piece $\langle k_T^2\rangle_{\rm evol}$, entirely to the evolution and independent of the profile $F^{\rm NP}$:

$$\langle k_\perp^2\rangle=\langle k_\perp^2\rangle_{\rm NP}+\langle k_\perp^2\rangle_{\rm evol},$$

$$\langle k_\perp^2\rangle_{\rm NP}=-4\left.\frac{dF^{\rm NP}(b)/db^2}{F^{\rm NP}(b)}\right|_{b=0},$$

$$\langle k_\perp^2\rangle_{\rm evol}=-4\left.\frac{df^{\rm evol}(b,x,Q)/db^2}{f^{\rm evol}(b,x,Q)}\right|_{b=0}. \tag{10.1}$$

The contribution $\langle k_T^2\rangle_{\rm NP}$ has already been discussed in Sec. IV; hence, here, we analyze the term generated by the evolution.

Let us denote

$$f_j^{(1)}(x,Q)\equiv\left.\frac{df_j^{\rm evol}(b,x,Q)}{db^2}\right|_{b=0}. \tag{10.2}$$

In Mellin space, the equations obtained by expanding Eq. (3.4) up to first order in b^2 around $b=0$ read

$$\frac{df_{\rm NS}^{(1)}(n,Q)}{dQ^2}=-\frac{\alpha_S(Q^2)}{8\pi Q^2}[\gamma_{n,NS}^{(0)}f_{\rm NS}^{(1)}(n,Q)+Q^2\gamma_{n,NS}^{(1)}f_{\rm NS}(n,0,Q)] \tag{10.3}$$

and

$$\frac{df_S^{(1)}(n,Q)}{dQ^2}=-\frac{\alpha_S(Q^2)}{8\pi Q^2}\{\gamma_{n,qq}^{(0)}f_S^{(1)}(n,Q)+\gamma_{n,qG}^{(0)}f_G^{(1)}(n,Q)+Q^2[\gamma_{n,qq}^{(1)}f_S(n,0,Q)+\gamma_{n,qG}^{(1)}f_G(n,0,Q)]\}, \tag{10.4}$$

$$\frac{df_G^{(1)}(n,Q)}{dQ^2}=-\frac{\alpha_S(Q^2)}{8\pi Q^2}\{\gamma_{n,Gq}^{(0)}f_S^{(1)}(n,Q)+\gamma_{n,GG}^{(0)}f_G^{(1)}(n,Q)+Q^2[\gamma_{n,Gq}^{(1)}f_S(n,0,Q)+\gamma_{n,GG}^{(1)}f_G(n,0,Q)]\}, \tag{10.5}$$

which form a set of ordinary inhomogeneous differential equations. Since at the scale Q_0 all the width is by construction generated by the initial profile F, the initial conditions for Eqs. (10.3), (10.6) are

$$f_j^{(1)}(n,Q_0)=0. \tag{10.6}$$

For the nonsinglet case we have the solution

$$f_{\rm NS}^{(1)}(n,Q)=-\gamma_{n,NS}^{(1)}f_{\rm NS}(n,0,Q)r_1(Q_0^2,Q^2). \tag{10.7}$$

In the singlet channel we carry the analysis numerically.

Next, we pass to x space via the numerical inverse Mellin transform. The results for the dynamically generated root-mean-squared radius of the pion are shown in Fig. 6 for various values of x. In confirmation of the results of Ref. [16], we note that the $k_\perp$ width increases with Q for all parton species. The width for the gluons (solid lines) is larger than the width of the nonsinglet (valence) quarks (dashed lines) and the singlet quarks (dotted lines). With the log-log scales of Fig. 6 the slopes of the plotted lines become to a good approximation equal to one another at large Q^2.

With the help of previously derived expressions for the behavior of $f_{\rm NS}$ near $x=0$ and $x=1$ we may obtain the following expressions $\langle k_\perp^2\rangle_{\rm NS}^{\rm evol}$ near the end points. From Eq. (8.8) we have, at $x\to 0$,

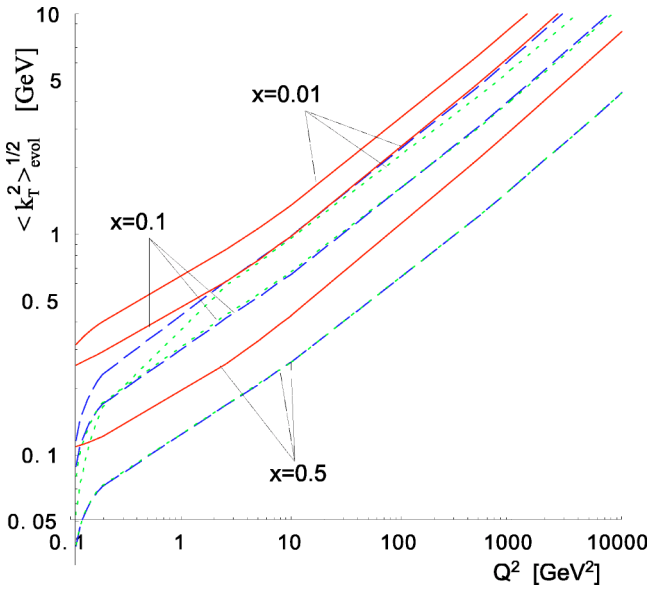

FIG. 6. The rms transverse momenta of UPDs of the pion for $x=0.01$, 0.1, and 0.5, plotted as functions of the renormalization scale Q^2. Solid lines: gluons. Dashed lines: nonsinglet quarks. Dotted lines: singlet quarks.

$$\langle k_\perp^2\rangle_{\rm NS}^{\rm evol}\to \frac{I_1(\sqrt{-4C_F r_0\log x})}{I_0(\sqrt{-4C_F r_0\log x})}\sqrt{-\frac{C_F\log x}{r_0}}r_1$$
$$\sim\sqrt{-\frac{C_F\log x}{r_0}}r_1. \tag{10.8}$$

At large Q^2 the leading behavior is

$$\langle k_\perp^2\rangle_{\rm NS}^{\rm evol}\to \sqrt{\frac{2\beta_0^{(4)}C_F\log\frac{1}{x}}{\log\frac{\alpha(\mu_c^2)}{\alpha(Q^2)}}\frac{\alpha(Q^2)}{8\pi}}Q^2; \tag{10.9}$$

i.e., up to the $\log\log Q^2$ corrections the spreading proceeds with $\alpha(Q^2)Q^2$. At $x\to 1$ we find from Eq. (8.6) that

$$\langle k_\perp^2\rangle_{\rm NS}^{\rm evol}\to \frac{2C_F(1-x)^2 r_1}{(1+8C_F r_0)(2+8C_F r_0)}. \tag{10.10}$$

At large Q^2 the leading behavior is

$$\langle k_\perp^2\rangle_{\rm NS}^{\rm evol}\to \frac{\beta_0^{(4)2}(1-x)^2\alpha(Q^2)}{64\pi C_F\left[\log\frac{\alpha(\mu_c^2)}{\alpha(Q^2)}\right]^2}Q^2. \tag{10.11}$$

Again, the growth is, up to the $\log\log Q^2$ corrections, proportional to $\alpha(Q^2)Q^2$.

For the gluons the same asymptotic behavior of $\langle k_\perp^2\rangle_{\rm G}^{\rm evol}$ follows from Eq. (9.6). Thus, to summarize, all UPDs grow at large Q as $Q^2\alpha(Q^2)$, in accordance to the behavior in Fig. 6.

Interestingly, it can be noticed from Fig. 6 that at $Q\to Q_0^+$ the $k_\perp$ width for the gluons does not vanish. In this limit both $f_G^{\rm evol}(x,0,Q)$ and $f_G^{(1)}(x,Q)$ vanish, as is obvious from Eqs. (4.2), (10.6). Thus one has a 0/0 limit. From Eqs. (2.4), (10.3) with the initial condition (4.3), (10.6) one can easily obtain that

$$\lim_{Q\to Q_0}\langle k_\perp^2\rangle_G^{\rm evol}=Q_0\frac{\int_x^1 dz P_{Gq}(z)\frac{(1-z)^2}{z}}{\int_x^1 dz P_{Gq}(z)\frac{1}{z}}$$
$$=Q_0\frac{x^4-6x^3+21x^2-18x\log x-10x-6}{3(x^2-2x\log x+x-2)}, \tag{10.12}$$

which is positive for $x\in[0,1)$ and equal to 0 for $x=1$. On the other hand, since for the quarks $f_{NS,S}^{\rm evol}(x,0,Q)\neq 0$, $\langle k_\perp^2\rangle_{NS,S}^{\rm evol}$ vanish at Q_0.

In phenomenological applications it is sometimes useful to have a simple formula characterizing the discussed behavior. In the range $2\ {\rm GeV}^2<Q^2<10\,000\ {\rm GeV}^2$ and $0.005<x<0.8$ the following simpleminded interpolating formula works to within a few percent:

$$(\langle k_\perp^2\rangle_i^{\rm evol})^{1/2}=A_i\left(\log\frac{1}{x}\right)\left(\frac{Q^2}{\Lambda_{\rm QCD}^2}\right)^{0.35+0.004\log(Q^2/\Lambda_{\rm QCD}^2)}, \tag{10.13}$$

where $i=$ NS, S, or G, and

$$A_{\rm NS}(y)=-0.017y^{1/2}+0.113y-0.057y^{3/2}+0.010y^2,$$
$$A_S(y)=-0.021y^{1/2}+0.120y-0.059y^{3/2}+0.009y^2,$$
$$A_G(y)=-0.016y^{1/2}+0.150y-0.075y^{3/2}+0.011y^2. \tag{10.14}$$

The power of Q^2 of 0.35 in Eq. (10.13), rather than 1/2 corresponding to $\langle k_\perp^2\rangle_i^{\rm evol}\sim Q^2\alpha(Q^2)$, compensates, in the chosen range for Q, for the logarithmic corrections. We note that Eq. (10.13) holds for the pion with the initial conditions (4.16) provided by the chiral quark models.

XI. FORMAL LIMITS FOR OTHER INITIAL CONDITIONS

Certain formal results listed in this paper, such as the formulas for the nonsinglet quarks, Eqs. (7.5), (7.6), (8.7), (8.8), (9.2), (10.8), (10.9), are specific to the evolution with the initial condition following from the chiral quark models, Eqs. (4.4), (4.16). However, these results can be easily generalized. Note that most of the popular parametrizations of initial conditions, such as those of Refs. [53,54], involve linear combinations of $x^\alpha(1-x)^\beta$. It is understood that the factorization in the initial condition between x and b variable holds, as assumed in Ref. [16].

For the case of large-b asymptotics, the relevant formula is Eq. (7.4). With the initial condition $x^\alpha(1-x)^\beta$ it becomes

$$\int_C \frac{dn}{2\pi i} x^{-n} \frac{e^{y_0+y_1 n}}{n+\alpha} = x^\alpha e^{y_0-\alpha y_1} \Theta\left(y_1 + \log\frac{1}{x}\right), \tag{11.1}$$

and expressions (7.5), (7.6) are modified accordingly, with x replaced by x^α and y_1 in the exponent multiplied by α. The formulas (7.8) remain valid. Therefore the power-law behavior at large b is independent of the initial condition and is $b^{-8C_F r_0(Q_0^2,Q^2)}$ for the quarks and $b^{-8N_c r_0(Q_0^2,Q^2)}$ for the gluons.

In the limit of $x\to 1$ the only difference is the appearance of the extra power of β in the in Eq. (8.7). Thus, the UPDs for finite b approach the $b=0$ case of the integrated distributions as $(1-x)^2$.

In the limit of $x\to 0$ we need generalizations of the Mellin transforms of Eqs. (9.1), (9.6) for $\alpha\neq 1$. These are

$$\begin{aligned}
&\int_C dn x^{-n} \frac{1}{n+\alpha} \exp\left(\frac{a}{n+1}\right) \\
&= x\sum_{k=0}^{\infty} (-1)^k (\alpha-1)^k \left(\frac{\log\frac{1}{x}}{a}\right)^{k/2} I_k\left(2\sqrt{a\log\frac{1}{x}}\right) \\
&\sim \frac{x\exp\left(2\sqrt{a\log\frac{1}{x}}\right)}{(\alpha-1)\sqrt{4\pi\sqrt{a\log\frac{1}{x}}}\sqrt{\frac{\log\frac{1}{x}}{a}}}, \\
&\alpha\neq 1,\ a>0,
\end{aligned} \tag{11.2}$$

and

$$\begin{aligned}
&\int_C dn x^{-n} \frac{1}{n+\alpha} \exp\left(\frac{a}{n}\right) \\
&= \sum_{k=0}^{\infty} (-1)^k \alpha^k \left(\frac{\log\frac{1}{x}}{a}\right)^{k/2} I_k\left(2\sqrt{a\log\frac{1}{x}}\right) \\
&\sim \frac{\exp\left(2\sqrt{a\log\frac{1}{x}}\right)}{\alpha\sqrt{4\pi\sqrt{a\log\frac{1}{x}}}\sqrt{\frac{\log\frac{1}{x}}{a}}}, \quad \alpha\neq 0,\ a>0.
\end{aligned} \tag{11.3}$$

The analogue of Eqs. (9.2), (9.7), (10.8), (10.9) follow straightforwardly. In particular, the $Q^2\alpha(Q^2)$ large-Q behavior for all parton distributions is preserved.

XII. CONCLUSIONS

We have presented a new method of solving the Kwieciński equations for the leading-order QCD evolution of unintegrated parton distributions. The method is based on the Mellin transform and parallels the standard analysis of the DGLAP equations. Our main results are as follows.

(1) We have found analytic forms of the b-dependent anomalous dimensions, expressed through hypergeometric functions, which allowed us to study formal aspects of the equations and their solutions—e.g., the asymptotic forms of the evolution-generated UPDs at large b or at $x\to 0$ and $x\to 1$. We have also demonstrated that the proposed numerical method is fast and stable.
(2) The numerical work can be simplified if low-b or large-b expansions are used.
(3) At large b the evolution-generated b-dependent UPDs exhibit a power-law falloff, with the magnitude of the exponents growing with the probing scale Q; cf. Eqs. (7.5), (7.8). The falloff is steeper for the gluons than for the quarks.
(4) At $x\to 0$ we have found generalizations of the DLLA behavior; cf. Eqs. (9.2), (9.7). We have also shown that for large b the solution for the valence UPD of the pion grows linearly with x for not too large x, and the slope decreases with b as a power law.
(5) At $x\to 1$ the evolution-generated b-dependent UPDs approach the integrated distributions as $(1-x)^2$.
(6) Our numerical results fully confirm the finding of Ref. [16], where a different numerical method was used. We find the spreading of the $k_\perp$ distributions with the probing scale Q, with the effect strongest for gluons and increasing with decreasing x. We have also shown that the widths $\langle k_\perp^2\rangle_i^{\rm evol}$ in all channels i increase at large Q^2 as $Q^2\alpha(Q^2)$.
(7) For practical purposes in possible phenomenological applications, we have parametrized $\langle k_\perp^2\rangle_i^{\rm evol}$ with a simple formula which works with accuracy of a few percent.

Although the specific study of this paper was devoted to the pion with the initial condition following from the chiral models, and several of the more detailed analytic formulas were specific to this case, the developed method is general and can be applied to any initial form of the data. In particular, it can be used with the GRS [53] or GRV [54] parametrization supplied by a profile in b, such as already studied in Ref. [16]. The formal results of Sec. XI are general for a wide class of initial conditions, suitable for both the pion and nucleon.

It should certainly be interesting to extend the present analysis of the UPDs to next-to-leading order, which would allow for a more accurate analysis. This work is in progress.

ACKNOWLEDGMENTS

We thank Krzysztof Golec-Biernat and Antoni Szczurek for useful discussions. One of us (W.B.) is grateful to Andrzej Horzela for pointing out the impressive col-

lection of practical mathematical knowledge at http://www.mathworld.com [63]. Support from DGI and FEDER funds, under contract BFM2002-03218, and by the Junta de Andalucía grant FM-225 and EURIDICE grant HPRN-CT-2003-00311 is acknowledged. Partial support from the Spanish Ministerio de Asuntos Exteriores and the Polish State Committee for Scientific Research, grant 07/2001-2002, is also gratefully acknowledged.

APPENDIX A: ELEMENTS OF THE PERTURBATIVE QCD EVOLUTION

We use the LO QCD evolution with three active flavors up to the scale $\mu_c^2=4\ \mathrm{GeV}^2$ and four active flavors above. Therefore $\alpha=g^2/(4\pi)$ is given by

$$\alpha(Q^2)=\frac{4\pi}{\beta_0^{(3)}\log\left(\frac{Q^2}{\Lambda^2_{QCD}}\right)},\quad Q^2\leqslant\mu_c^2,$$

$$\alpha(Q^2)=\frac{4\pi}{\beta_0^{(4)}\log\left(\frac{Q^2}{\Lambda_4^2}\right)},\quad Q^2>\mu_c^2,$$

$$\Lambda_4=\mu_c\left(\frac{\Lambda_{QCD}}{\mu_c}\right)^{\beta_0^{(3)}/\beta_0^{(4)}},\tag{A1}$$

with $\beta_0^{(N_f)}=11-2N_f/3$ for $N_c=3$, where N_f and N_c denote the number of flavors and colors, respectively. Along this paper we take

$$\Lambda_{\mathrm{QCD}}=226\ \ \mathrm{MeV},\tag{A2}$$

as was done in Refs. [42,45–47]. The value of the scale Λ_4 ensures matching at $Q^2=\mu_c^2$. Numerically, $\beta_0^{(3)}=9$, $\beta_0^{(4)}=25/3$, and $\Lambda_4=189$ MeV.

The functions r_k, defined in Eq. (6.1), have the explicit form

$$r_0(Q_0^2,Q^2)=\frac{1}{2\beta_0^{(3)}}\log\left(\frac{\log(Q^2/\Lambda^2_{\mathrm{QCD}})}{\log(Q_0^2/\Lambda^2_{\mathrm{QCD}})}\right)$$

$$=\frac{1}{2\beta_0^{(3)}}\log\frac{\alpha(Q_0^2)}{\alpha(Q^2)},\quad Q^2\leqslant\mu_c^2,$$

$$r_0(Q_0^2,Q^2)=r_0(Q_0^2,\mu_c^2)+\frac{1}{2\beta_0^{(4)}}\log\left(\frac{\log(Q^2/\Lambda_4^2)}{\log(\mu_c^2/\Lambda_4^2)}\right)$$

$$=r_0(Q_0^2,\mu_c^2)+\frac{1}{2\beta_0^{(4)}}\log\frac{\alpha(\mu_c^2)}{\alpha(Q^2)},\quad Q^2>\mu_c^2,\tag{A3}$$

and, for $k\neq 0$,

$$r_k(Q_0^2,Q^2)=\frac{\Lambda^{2k}_{\mathrm{QCD}}}{2\beta_0^{(3)}}\left[\mathrm{Li}\left(\frac{Q^{2k}}{\Lambda^{2k}_{\mathrm{QCD}}}\right)-\mathrm{Li}\left(\frac{Q_0^2}{\Lambda^2_{\mathrm{QCD}}}\right)\right],\quad Q^2\leqslant\mu_c^2,$$

$$r_k(Q_0^2,Q^2)=r_k(Q_0^2,\mu_c^2)+\frac{\Lambda_4^{2k}}{2\beta_0^{(4)}}\left[\mathrm{Li}\left(\frac{Q^{2k}}{\Lambda_4^{2k}}\right)-\mathrm{Li}\left(\frac{\mu_c^2}{\Lambda_4^2}\right)\right],\quad Q^2>\mu_c^2.\tag{A4}$$

Above we have used the indefinite integral

$$\int\frac{dQ^2Q^{2k}}{Q^2\log(Q^2/\Lambda^2)}=\Lambda^{2k}\mathrm{Li}\left(\frac{Q^{2k}}{\Lambda^{2k}}\right),\quad k=1,2,\ldots,\tag{A5}$$

where the logarithmic integral is

$$\mathrm{Li}(x)=\int_0^x dt/\log t.\tag{A6}$$

At large Q^2,

$$\Lambda^{2k}\mathrm{Li}\left(\frac{Q^{2k}}{\Lambda^{2k}}\right)=Q^{2k}\left(\frac{1}{k\log\frac{Q^2}{\Lambda^2}}+\frac{1}{k^2\log^2\frac{Q^2}{\Lambda^2}}+\cdots\right).\tag{A7}$$

The functions $P_{ab}(z)$ are the LO splitting functions corresponding to real emission—i.e.,

$$P_{qq}(z)=C_F\frac{1+z^2}{1-z},$$

$$P_{qG}(z)=N_f[z^2+(1-z)^2],$$

$$P_{Gq}(z)=C_F\frac{1+(1-z)^2}{z},$$

$$P_{GG}(z)=2N_c\left[\frac{z}{1-z}+\frac{1-z}{z}+z(1-z)\right],\tag{A8}$$

with $C_F=(N_c^2-1)/(2N_c)=4/3$.

APPENDIX B: *b*-DEPENDENT ANOMALOUS DIMENSIONS

We introduce

$$u=\frac{Q^2b^2}{4},\tag{B1}$$

as well as the anomalous dimensions for the $b=0$ case of the DGLAP equations, where for the nonsinglet we have

$$\gamma^{(0)}_{n,NS}=2C_F\left(-3+\frac{2}{1+n}+\frac{2}{2+n}+4H_n\right), \tag{B2}$$

while for the singlet,

$$\gamma^{(0)}_{n,qq}=\gamma_{n,NS}(0),$$

$$\gamma^{(0)}_{n,qG}=-4N_f\left(\frac{1}{1+n}-\frac{2}{2+n}+\frac{2}{3+n}\right),$$

$$\gamma^{(0)}_{n,Gq}=-4C_F\left(\frac{2}{n}-\frac{2}{1+n}+\frac{1}{2+n}\right),$$

$$\gamma^{(0)}_{n,GG}=2N_c\left(-3-\frac{4}{n}+\frac{8}{1+n}-\frac{4}{2+n}+\frac{4}{3+n}+4H_n\right). \tag{B3}$$

The symbol H_n denotes the harmonic number

$$H_n=\sum_{k=1}^{n}\frac{1}{k}=\frac{\Gamma'(n+1)}{\Gamma(n+1)}+\gamma, \tag{B4}$$

which is a meromorphic function in the complex n variable, with poles located at negative integers $n=-1,-2,-3,\ldots$ and residues equal to -1.

Below we list the anomalous dimensions for the moments of the unintegrated parton distributions in b space, defined in Eq. (3.2). The formulas follow from the basic analytic integral

$$\frac{\Gamma(2+\mu+\nu)}{\Gamma(1+\mu)\Gamma(1+\nu)}\int_0^1 dy y^{\mu}(1-y)^{\nu}J_0(2\sqrt{uy}) = {}_2F_3\left(\frac{1+\mu}{2},\frac{2+\mu}{2};1,\frac{2+\mu+\nu}{2},\frac{3+\mu+\nu}{2};-u\right) \tag{B5}$$

and relations among the generalized hypergeometric functions. For the nonsinglet case we have

$$\gamma_{n,NS}(Qb)=\gamma^{(0)}_{n,NS}+\frac{4C_F}{(1+n)(2+n)}\left[-3-2n+2(2+n)\,{}_1F_2\left(\frac{1}{2};\frac{2+n}{2},\frac{3+n}{2};-u\right)-{}_1F_2\left(\frac{3}{2};\frac{3+n}{2},\frac{4+n}{2};-u\right)+2u\,{}_3F_4\left(1,1,\frac{3}{2};2,2,\frac{3+n}{2},\frac{4+n}{2};-u\right)\right], \tag{B6}$$

whereas for the singlet case,

$$\gamma_{n,qq}(Qb)=\gamma_{n,NS}(Qb),$$

$$\gamma_{n,qG}(Qb)=\gamma^{(0)}_{n,qG}+\frac{4N_f}{(1+n)(2+n)(3+n)(4+n)(5+n)}\left(-\left\{(4+n)(5+n)\left[-4-n(3+n)+(2+n)(3+n)\,{}_2F_1\left(\frac{1}{2};\frac{2+n}{2},\frac{3+n}{2};-u\right)-2(3+n)\,{}_1F_2\left(\frac{3}{2};\frac{3+n}{2},\frac{4+n}{2};-u\right)+4\,{}_1F_2\left(\frac{3}{2};\frac{4+n}{2},\frac{5+n}{2};-u\right)\right]\right\}+24u\,{}_1F_2\left(\frac{5}{2};\frac{6+n}{2},\frac{7+n}{2};-u\right)\right),$$

$$\gamma_{n,Gq}(Qb)=\gamma^{(0)}_{n,Gq}+\frac{4C_F}{n(1+n)(2+n)(3+n)(4+n)}\left\{-\left[(1+n)(2+n)(3+n)(4+n)\,{}_1F_2\left(\frac{1}{2};\frac{1+n}{2},\frac{2+n}{2};-u\right)\right]+(3+n)(4+n)\left[4+n(3+n)-2\,{}_1F_2\left(\frac{3}{2};\frac{3+n}{2},\frac{4+n}{2};-u\right)\right]+12u\,{}_1F_2\left(\frac{5}{2};\frac{5+n}{2},\frac{6+n}{2};-u\right)\right\},$$

$$\gamma_{n,GG}(Qb)=\gamma^{(0)}_{n,GG}+8N_c\Bigg[\frac{1}{n}-\frac{2}{1+n}+\frac{1}{2+n}-\frac{1}{3+n}+\frac{{}_1F_2\left(\frac{1}{2};1+\frac{n}{2},\frac{3}{2}+\frac{n}{2};-u\right)}{1+n}-\frac{{}_1F_2\left(\frac{3}{2};1+\frac{n}{2},\frac{3}{2}+\frac{n}{2};-u\right)}{n+n^2}$$
$$-\frac{{}_1F_2\left(\frac{3}{2};\frac{3}{2}+\frac{n}{2},2+\frac{n}{2};-u\right)}{(1+n)(2+n)}+\frac{2\,{}_1F_2\left(\frac{3}{2};2+\frac{n}{2},\frac{5}{2}+\frac{n}{2};-u\right)}{(1+n)(2+n)(3+n)}-\frac{12u\,{}_1F_2\left(\frac{5}{2};3+\frac{n}{2},\frac{7}{2}+\frac{n}{2};-u\right)}{(1+n)(2+n)(3+n)(4+n)(5+n)}$$
$$+\frac{u\,{}_3F_4\left(1,1,\frac{3}{2};2,2,\frac{3}{2}+\frac{n}{2},2+\frac{n}{2};-u\right)}{(1+n)(2+n)}\Bigg]. \tag{B7}$$

One may verify that the analyticity properties in n of the anomalous dimensions (B6), (B7) are the same as for the $b=0$ case of Eqs. (B2), (B4).

APPENDIX C: EXPANSION OF ANOMALOUS DIMENSIONS AT LOW bQ

We may expand in the anomalous dimensions in powers of Q^2b^2,

$$\gamma_{n,j}(Qb)=\gamma^{(0)}_{n,j}+\gamma^{(1)}_{n,j}Q^2b^2+\cdots, \tag{C1}$$

which yields

$$\gamma^{(1)}_{n,NS}=\gamma^{(1)}_{n,qq}=\frac{2C_F(n^2+5n+7)}{(n+1)(n+2)(n+3)(n+4)},$$
$$\gamma^{(1)}_{n,qG}=\frac{2N_f(n^2+3n+14)}{(n+1)(n+2)(n+3)(n+4)},$$
$$\gamma^{(1)}_{n,Gq}=\frac{2C_F(n^2+7n+24)}{(n+1)(n+2)(n+3)(n+4)},$$
$$\gamma^{(1)}_{n,GG}=\frac{2N_c[n(n+5)(n^2+5n+16)+120]}{n(n+1)n+2)(n+3)(n+4)(n+5)}. \tag{C2}$$

More generally, introducing the Euler beta function $\mathsf{B}(x,y)=\Gamma(x)\Gamma(y)/\Gamma(x+y)$ and applying the series expansion of the Bessel function,

$$J_0(x)=\sum_{k=0}^{\infty}\frac{(-x^2)^k}{2^k k!^2}, \tag{C3}$$

we arrive at the expansion formulas

$$\gamma_{n,NS}(Qb)=\gamma_{n,qq}(Qb)=\gamma^{(0)}_{n,qq}-C_F\sum_{k=1}^{\infty}\frac{(-Q^2b^2)^k4^{1-k}}{k!^2}$$
$$\times[\mathsf{B}(2k,n+1)+\mathsf{B}(2k,n+3)],$$

$$\gamma_{n,qG}(Qb)=\gamma^{(0)}_{n,qG}-N_f\sum_{k=1}^{\infty}\frac{(-Q^2b^2)^k4^{1-k}}{k!^2}$$
$$\times[\mathsf{B}(2k+1,n+1)-2\mathsf{B}(2k+1,n+2)$$
$$+2\mathsf{B}(2k+1,n+3)],$$

$$\gamma_{n,Gq}(Qb)=\gamma^{(0)}_{n,Gq}-C_F\sum_{k=1}^{\infty}\frac{(-Q^2b^2)^k4^{1-k}}{k!^2}$$
$$\times[2\mathsf{B}(2k+1,n)-2\mathsf{B}(2k+1,n+1)$$
$$+\mathsf{B}(2k+1,n+2)],$$

$$\gamma_{n,GG}(Qb)=\gamma^{(0)}_{n,GG}-2N_c\sum_{k=1}^{\infty}\frac{(-Q^2b^2)^k4^{1-k}}{k!^2}[\mathsf{B}(2k,n+2)$$
$$+\mathsf{B}(2k+2,n)+\mathsf{B}(2k+2,n+2)]. \tag{C4}$$

APPENDIX D: ASYMPTOTICS OF THE ANOMALOUS DIMENSIONS AT LARGE bQ

We may use the asymptotic forms of the generalized hypergeometric functions appearing in Eqs. (B6), (B7). One has [64]

$${}_1F_2\left(a_1;b_1,b_2;-\frac{Q^2b^2}{4}\right)$$
$$=\frac{\Gamma(b_1)\Gamma(b_2)}{\Gamma(b_1-a_1)\Gamma(b_2-a_1)}\left(\frac{4}{Q^2b^2}\right)^{a_1}$$
$$+\frac{\Gamma(b_1)\Gamma(b_2)}{\sqrt{\pi}\Gamma(a_1)}\left\{\cos(Qb-\pi c_1)\right.$$
$$\left.+\frac{c_2}{Qb}\sin(Qb-\pi c_1)\right\}\left(\frac{4}{Q^2b^2}\right)^{c_1}+\cdots,$$

$$c_1=\frac{1}{2}\left(b_1+b_2-a_1-\frac{1}{2}\right),$$

$$c_2=\frac{1}{8}(12a_1^2-8(b_1+b_2+1)a_1$$

$$-4(b_1-b_2)^2+8(b_1+b_2)-3), \tag{D1}$$

and [65]

$${}_3F_4\left(1,1,\frac{3}{2};2,2,\frac{n+3}{2},\frac{n+4}{2};-\frac{Q^2b^2}{4}\right)$$
$$=\frac{4(n+1)(n+2)}{nQ^3b^3}\left(Qb\left[n\log\frac{Qb}{2}-n\psi^0(n)-1\right]+n^2\right)$$
$$+\frac{8\Gamma(n+3)}{\sqrt{2\pi}}\cos\left(Qb-\frac{2n+3}{4}\pi\right)(Qb)^{-n/2-7/2}$$
$$+\cdots. \tag{D2}$$

Then the following asymptotic expansions for the b-dependent anomalous dimensions hold:

$$\gamma_{\rm NS}(n,Qb)$$
$$=\gamma_{qq}(n,Qb)$$
$$=4C_F\left\{\log\frac{Q^2b^2}{4}+2\gamma-\frac{3}{2}+\frac{2n+2}{Qb}\right.$$
$$+\frac{\Gamma(n+1)(Qb)^{-n-5/2}}{4\sqrt{2\pi}}\left[24bQ\cos\left(\frac{2n+3}{4}\pi-Qb\right)\right.$$
$$\left.\left.-(12n+13)\sin\left(\frac{2n+3}{4}\pi-Qb\right)\right]\right\}+\cdots, \tag{D3}$$

$$\gamma_{qG}(n,Qb)$$
$$=4N_f\left\{-\frac{1}{Qb}+\frac{\Gamma(n+1)(Qb)^{-n-5/2}}{8\sqrt{\pi}}\right.$$
$$\times\left[(-12n+8Qb-11)\cos\left(\frac{n\pi}{2}-Qb\right)\right.$$
$$\left.\left.+(12n+8Qb+11)\sin\left(\frac{n\pi}{2}-Qb\right)\right]\right\}+\cdots, \tag{D4}$$

$$\gamma_{Gq}(n,Qb)$$
$$=4C_F\left\{-\frac{1}{Qb}+\frac{\Gamma(n)(Qb)^{-n-3/2}}{4\sqrt{\pi}}\left[(4n+8Qb-1)\right.\right.$$
$$\left.\left.\times\cos\left(\frac{n\pi}{2}-Qb\right)+(4n-8Qb-1)\sin\left(\frac{n\pi}{2}-Qb\right)\right]\right\}$$
$$+\cdots, \tag{D5}$$

$$\gamma_{GG}(n,Qb)=\frac{4N_f}{3}+4N_c\left\{\log\frac{Q^2b^2}{4}+2\gamma-\frac{11}{6}+\frac{2n+2}{Qb}\right.$$
$$-\frac{4\Gamma(n)(Qb)^{-n-1/2}}{\sqrt{2\pi}}\cos\left(\frac{2n+1}{4}\pi-Qb\right)$$
$$+\frac{[\Gamma(n)-20\Gamma(n+1)](Qb)^{-n-3/2}}{4\sqrt{\pi}}$$
$$\left.\times\left[\cos\left(\frac{n}{2}\pi-Qb\right)+\sin\left(\frac{n}{2}\pi-Qb\right)\right]\right\}+\cdots. \tag{D6}$$

The ellipses denote terms subleading in $1/Qb$. The above formulas assume that n is kept fixed. In actual applications, such as numerical programming of the generalized hypergeometric functions, it is practical to switch from the general formulas (B6), (B7) to the asymptotic expressions (D3), (D6) when $Qb\geqslant 10|n|$.

APPENDIX E: POLE-RESIDUE EXPANSION OF THE ANOMALOUS DIMENSIONS

For $b\neq 0$ the analytic structure of the b-dependent anomalous dimensions remains the same as for $b=0$. This can be seen by expanding the Bessel function in the integrand of Eq. (3.2) as a power series around $z=0$, which yields

$$\gamma_{n,ab}(Qb)=-4\int_0^1 dz\sum_{k=0}^{\infty}\frac{1}{k!}[J_0^{(k)}(Qb)$$
$$\times(-Qb)^k z^{n+k}-1]P_{ab}(z). \tag{E1}$$

Applying the trick

$$1=J_0(0)=-4\sum_{k=0}^{\infty}\frac{1}{k!}J_0^{(k)}(Qb)(-Qb)^k, \tag{E2}$$

we find the expansion involving index-shifted anomalous dimensions at $b=0$—namely,

$$\gamma_{n,ab}(Qb)=\sum_{k=0}^{\infty}\frac{(-Qb)^k}{k!}J_0^{(k)}(Qb)\,\gamma_{n+k,ab}(0). \tag{E3}$$

Using the explicit expression for the anomalous dimension this series may be rewritten as a pole-residue expansion

$$\gamma_{n,ab}(Qb)=\sum_{k=0}^{\infty}\frac{R_k^{ab}(Qb)}{n+k}. \tag{E4}$$

In practice this means that the Mellin contour used in the case of $b=0$ can be used in the $b\neq 0$ case as well. In the nonsinglet case the first few residues read

$$\begin{aligned}
R_1^{\rm NS}(A)&=-4C_F J_0(A),\\
R_2^{\rm NS}(A)&=-4C_F[J_0(A)+AJ_1(A)],\\
R_3^{\rm NS}(A)&=-2C_F[-(A^2-4)J_0(A)+3AJ_1(A)],
\end{aligned} \tag{E5}$$

while in the singlet channel $R_i^{qq}=R_i^{\rm NS}$ and

$$\begin{aligned}
R_1^{qG}(A)&=-4N_F J_0(A),\\
R_2^{qG}(A)&=-4N_F[-2J_0(A)+AJ_1(A)],\\
&\cdots\\
R_0^{Gq}(A)&=-8C_F J_0(A),\\
R_1^{Gq}(A)&=-8C_F[-J_0(A)+AJ_1(A)],\\
&\cdots\\
R_0^{GG}(A)&=-8N_c J_0(A),\\
R_1^{GG}(A)&=-8N_c[-J_0(A)+AJ_1(A)].
\end{aligned} \tag{E6}$$

The pole-residue expansion controls the behavior of the solutions of Eq. (2.4) at low x. Since the subsequent residues carry powers of $A^n=(Qb)^n$, the expansion cannot be used for Qb too large.

[1] Yu.L. Dokshitzer, D.I. Dyakonov, and S.I. Troyan, Phys. Rep. **58**, 269 (1980).
[2] N. Nakamura, G. Pancheri, and Y.N. Srivastava, Z. Phys. C **21**, 243 (1984); A. Corsetti, A. Grau, G. Pancheri, and Y.N. Srivastava, Phys. Lett. B **382**, 282 (1996); A. Grau, G. Pancheri, and Y.N. Srivastava, Phys. Rev. D **60**, 114020 (1999).
[3] G. Sterman, ''Partons, factorization and resummation TASI 95,'' based on seven lectures at the Theoretical Advanced Study Institute, ''QCD and Beyond,'' Boulder, CO, 1995, hep-ph/9606312.
[4] M.A. Kimber, A.D. Martin, and M.G. Ryskin, Eur. Phys. J. C **12**, 655 (2000).
[5] M.A. Kimber, A.D. Martin, J. Kwieciński, and A.M. Staśto, Phys. Rev. D **62**, 094006 (2000).
[6] M.A. Kimber, A.D. Martin, and M.G. Ryskin, Phys. Rev. D **63**, 114027 (2001).
[7] A.D. Martin and M.G. Ryskin, Phys. Rev. D **64**, 094017 (2001).
[8] V.A. Khoze, A.D. Martin, and M.G. Ryskin, Eur. Phys. J. C **14**, 525 (2000); **19**, 477 (2001); **20**, 599(E) (2001).
[9] G. Watt, A.D. Martin, and M.G. Ryskin, Eur. Phys. J. C **31**, 73 (2003).
[10] G. Gustafson, L. Lönnblad, and G. Miu, J. High Energy Phys. **09**, 005 (2002).
[11] J.C. Collins, Acta Phys. Pol. B **34**, 3103 (2003).
[12] A. Szczurek, Acta Phys. Pol. B **34**, 3191 (2003).
[13] A.D. Martin and M.G. Ryskin, Phys. Rev. D **64**, 094017 (2001).
[14] J. Kwieciński, Acta Phys. Pol. B **33**, 1809 (2002).
[15] A. Gawron and J. Kwieciński, Acta Phys. Pol. B **34**, 133 (2003).
[16] A. Gawron, J. Kwieciński, and W. Broniowski, Phys. Rev. D **68**, 054001 (2003).
[17] M. Ciafaloni, Nucl. Phys. **B296**, 49 (1988).
[18] S. Catani, F. Fiorani, and G. Marchesini, Phys. Lett. B **234**, 339 (1990).
[19] S. Catani, F. Fiorani, and G. Marchesini, Nucl. Phys. **B336**, 18 (1990).
[20] G. Marchesini, Nucl. Phys. **B445**, 49 (1995).
[21] H. Jung, Mod. Phys. Lett. A **19**, 1 (2004).
[22] A. Gawron and J. Kwiecinski, hep-ph/0309303.
[23] J. Kwieciński and A. Szczurek, Nucl. Phys. **B680**, 164 (2004).
[24] M. Hansson, H. Jung, and L. Jonsson, hep-ph/0402019.
[25] L. Motyka and N. Timneanu, Eur. Phys. J. C **27**, 73 (2003).
[26] N.P. Zotov, A.V. Lipatov, and V.A. Saleev, Yad. Fiz. **66**, 786 (2003) [Phys. At. Nucl. **66**, 755 (2003)].
[27] A.V. Lipatov and N.P. Zotov, hep-ph/0304181.
[28] G. Watt, A.D. Martin, and M.G. Ryskin, Eur. Phys. J. C **31**, 73 (2003).
[29] A. Szczurek, Acta Phys. Pol. B **35**, 161 (2004).
[30] T.S. Biro and B. Muller, Phys. Lett. B **578**, 78 (2004).
[31] P. Levai, G. Papp, G.G. Barnafoldi, and G. Fai, nucl-th/0306019.
[32] A.V. Kotikov, A.V. Lipatov, and N.P. Zotov, hep-ph/0403135.
[33] A.V. Kotikov, A.V. Lipatov, G. Parente, and N.P. Zotov, Eur. Phys. J. C **26**, 51 (2002).
[34] J. Kwieciński and B. Ziaja, Phys. Rev. D **60**, 054004 (1999).
[35] J. Kwieciński and B. Ziaja, Phys. Rev. D **63**, 054022 (2001).
[36] A.I. Shoshi, F.D. Steffen, H.G. Dosch, and H.J. Pirner, Phys. Rev. D **66**, 094019 (2002).
[37] V. Gribov and L. Lipatov, Sov. J. Nucl. Phys. **15**, 438 (1972); **15**, 675 (1972).
[38] L. Lipatov, Sov. J. Nucl. Phys. **20**, 94 (1975).
[39] G. Altarelli and G. Parisi, Nucl. Phys. **B126**, 298 (1977).
[40] Y. Dokshitser, Sov. Phys. JETP **46**, 641 (1977).
[41] E. Ruiz Arriola, in *Proceedings of the Workshop on Lepton Scattering, Hadrons and QCD*, Adelaide, Australia, 2001, edited by W. Melnitchouk, A.W. Schreiber, A.W. Thomas, and P.C. Tandy (World Scientific, Singapore, 2001).
[42] E. Ruiz Arriola and W. Broniowski, Phys. Rev. D **67**, 074021 (2003).
[43] E. Ruiz Arriola and W. Broniowski, in Proceedings of Light

Cone Physics: Hadrons and Beyond, IPPP, University of Durham, UK, 2003, edited by S. Dalley, p. 166, hep-ph/0310044.

[44] For reviews see, e.g., U. Vogl and W. Weise, Prog. Part. Nucl. Phys. **27**, 195 (1991); S.P. Klevansky, Rev. Mod. Phys. **64**, 649 (1992); M.K. Volkov, Part Nuclei B **24**, 1 (1993); T. Hatsuda and T. Kunihiro, Phys. Rep. **247**, 221 (1994); Chr.V. Christov, A. Blotz, H.-C. Kim, P. Pobylitsa, T. Watabe, T. Meissner, E. Ruiz Arriola, and K. Goeke, Prog. Part. Nucl. Phys. **37**, 91 (1996); R. Alkofer, H. Reinhardt, and H. Weigel, Phys. Rep. **265**, 139 (1996); G. Ripka, *Quarks Bound by Chiral Fields* (Oxford Science, Oxford, 1997), and references therein.

[45] R.M. Davidson and E. Ruiz Arriola, Acta Phys. Pol. B **33**, 1791 (2002).

[46] R.M. Davidson and E. Ruiz Arriola, Phys. Lett. B **348**, 163 (1995).

[47] H. Weigel, E. Ruiz Arriola, and L.P. Gamberg, Nucl. Phys. **B560**, 383 (1999).

[48] E. Ruiz Arriola, Acta Phys. Pol. B **33**, 4443 (2002).

[49] E. Ruiz Arriola and W. Broniowski, Phys. Rev. D **66**, 094016 (2002).

[50] W. Broniowski and E. Ruiz Arriola, Phys. Lett. B **574**, 57 (2003).

[51] S. Noguera, L. Theußl, and V. Vento, Eur. Phys. J. A **20**, 483 (2004).

[52] A. De Rujula, S.L. Glashow, H.D. Politzer, S.B. Treiman, F. Wilczek, and A. Zee, Phys. Rev. D **10**, 1649 (1974).

[53] M. Glück, E. Reya, and I. Schienbein, Eur. Phys. J. C **10**, 313 (1999).

[54] M. Glück, E. Reya, and A. Vogt, Eur. Phys. J. C **5**, 461 (1998).

[55] E. Ruiz Arriola, Nucl. Phys. **A641**, 461 (1998).

[56] M. Glück and E. Reya, Nucl. Phys. **B130**, 76 (1977).

[57] M. Glück, E. Reya, and A. Vogt, Z. Phys. C **48**, 471 (1990).

[58] P.J. Sutton, A.D. Martin, R.G. Roberts, and W.J. Stirling, Phys. Rev. D **45**, 2349 (1992).

[59] W. Broniowski and E. Ruiz Arriola, Proceedings of Light Cone Physics: Hadrons and Beyond, IPPP, University of Durham, UK, 2003, edited by S. Dalley, p. 166, hep-ph/0310048.

[60] J.S. Conway *et al.*, Phys. Rev. D **39**, 92 (1989).

[61] A. Peterman, Phys. Rep. **53**, 157 (1979).

[62] K. Golec-Biernat, ''Deep inelastic scattering at small values of the Bjorken variable *x*,'' habilitation thesis, INP Cracow Report No. 1877/PH, 2001, http://www.ifj.edu.pl/reports/1877.pdf

[63] http://www.mathworld.com

[64] http://functions.wolfram.com/HypergeometricFunctions/Hypergeometric1F2/06/02/04

[65] http://functions.wolfram.com/HypergeometricFunctions/HypergeometricPFQ/06/04